9

Bias Adjustment for Singapore Climate Projections

Authors:
Chen Chen, Aurel Florian Moise, Sandeep Sahany, Muhammad Eeqmal Hassim, Xin Rong Chua, Venkatraman Prasanna, Gerald Lim, Shao-Yi Lee, Jianjun Yu, Anupam Kumar, Pavan Harika Raavi, Fei Luo

Meteorological Service Singapore
Centre for Climate Research Singapore

9.1 Introduction

The main objective of the V3 study is to generate accurate and realistic future climate projections in order to assess and adapt to the impacts of climate change in Singapore. To achieve this, a subset of the latest and most advanced CMIP6 GCMs that exhibit good performance over Southeast Asia has been carefully chosen to drive the regional dynamical downscaling simulations.

Despite improvements made in both the global models and the regional climate model SINGV-RCM, there are still residual biases present in the simulations, as shown in the evaluation chapter of the dynamical downscaling process (Chapter 7). In order to enhance the reliability of the climate change projections, it is necessary to adjust these biases. To achieve this, we conducted bias adjustments (BA) of the V3 downscaled simulations using the widely recognized ISIMIP3 bias adjustment method (Lange, 2019). We also performed rigorous methodology evaluations. The aim was to ensure that the adjusted outcomes effectively reduced biases and were physically realistic. This adjustment process plays a crucial role in producing more accurate and dependable climate projections, which are essential for addressing climate change impacts in Singapore.

By conducting bias adjustment of the V3 downscaled simulations, we aim to refine the results and ensure they align more closely with observed data. Here we used the following references: (1) For precipitation, we utilized a newly developed krigged rainfall dataset for Singapore. (2) For other variables, we utilized the latest version of high-resolution ERA5-driven simulation dataset (ERA5-RCM). This dataset underwent careful evaluation and was found suitable for our bias adjustment purposes.

In the data section, we will provide detailed information about the reference data and the model outputs used in our study. We will outline the sources and characteristics of the reference data as well as the specific model outputs from RCMs.

In the methods section, we will elaborate on the specific configurations we utilized for each variable. These configurations have undergone thorough evaluation using pseudo reality experiments and have consistently yielded realistic outcomes. We will explain the methodology and approaches employed to ensure the reliability and accuracy of our results.

Finally, in the results section, we will present the findings of the bias adjustment process for the model simulations, both in the historical period and in the future projections. Our bias adjustment techniques have demonstrated a very good performance. By applying these bias adjustments, we obtain more realistic RCM outputs, which are essential for conducting climate impact studies in the context of Singapore.

Table 9.1: List of downscaling simulations driven by sub-selected CMIP6 models

CMIP6 model	Ensemble ID	ECS (K)	GCM Resolution	RCM Resolution
ACCESS-CM2	r4i1p1f1	4.66	250km	8km, 2km
EC-Earth3	r1i1p1f1	4.26	100km	8km, 2km
MIROC6	r1i1p1f1	2.60	250km	8km
MPI-ESM1-2-HR	r1i1p1f1	2.98	100km	8km, 2km
NorESM2-MM	r1i1p1f1	2.49	100km	8km, 2km
UKESM1-0-LL	r1i1p1f2	5.36	250km	8km, 2km

9.2 Data

9.2.1 Simulations for bias adjustments

In our study, we performed bias adjustments for regional climate model (RCM) downscaling simulations driven by six CMIP6 global climate models (GCMs) as shown in Table 9.1. It is worth noting that the downscaling simulation using the MIROC6 GCM was conducted only for the 8km resolution.

Considering the availability of regional downscaling data (Table 9.2), we selected the 20-year period from 1995 to 2014 as the historical base period for our analysis. This time frame allows us to capture a representative snapshot of the recent past and establish a

baseline for comparison. For future projections, we focused on a 20-year period near the end of the 21st century to address the change, specifically from 2080 to 2099. By selecting these specific historical and future periods, we aimed to analyze and assess the changes in climate variables and their impacts over Singapore, providing valuable insights for climate change adaptation and planning in the region.

Table 9.2: Time period for model simulations

Scenarios	RCM @8km (SEA domain)	RCM @2km (WMC domain)
Historical	1955-2014 (60 yr)	1995-2014 (20 yr)
Future (SSP126)	2015-2099 (85 yr)	2040-2059 (20 yr), 2080-2099 (20 yr)
Future (SSP245)	2015-2099 (85 yr)	2040-2059 (20 yr), 2080-2099 (20 yr)
Future (SSP585)	2015-2099 (85 yr)	2040-2059 (20 yr), 2080-2099 (20 yr)

9.2.2 Domain for bias adjustments

In our study, we defined three specific regions for analysis: the South East Asia domain (SEA), the West Maritime Continent domain (WMC), and Singapore (SG) (Table 9.3). These regions are depicted in Figure 9.1 as D1 and D2 for SEA and WMC, respectively, and Figure 9.2 represents the SG domain. For the purpose of bias correction, we focused on conducting the adjustments specifically for the model simulations over the SG domain. To calculate Singapore-averaged results, we applied a landsea mask. This process enabled us to derive Singapore-specific climate information and assess the impacts of climate change on the country.

Table 9.3: List of defined domains

Domain	Latitude and Longitude	Grid info for 8km (lon) x (lat)	Grid info for 2km (lon) x (lat)	Remarks
SEA	18S-26N, 80W-160W	1120 x 560	N/A	8km model domain D1
WMC	7S-10N, 93-110W	237 x 236	936 x 943	2km model domain D2
SG	1.1N-1.54N, 103.5W-104.15W	10 x 7	36 x 24	bias adjustment domain

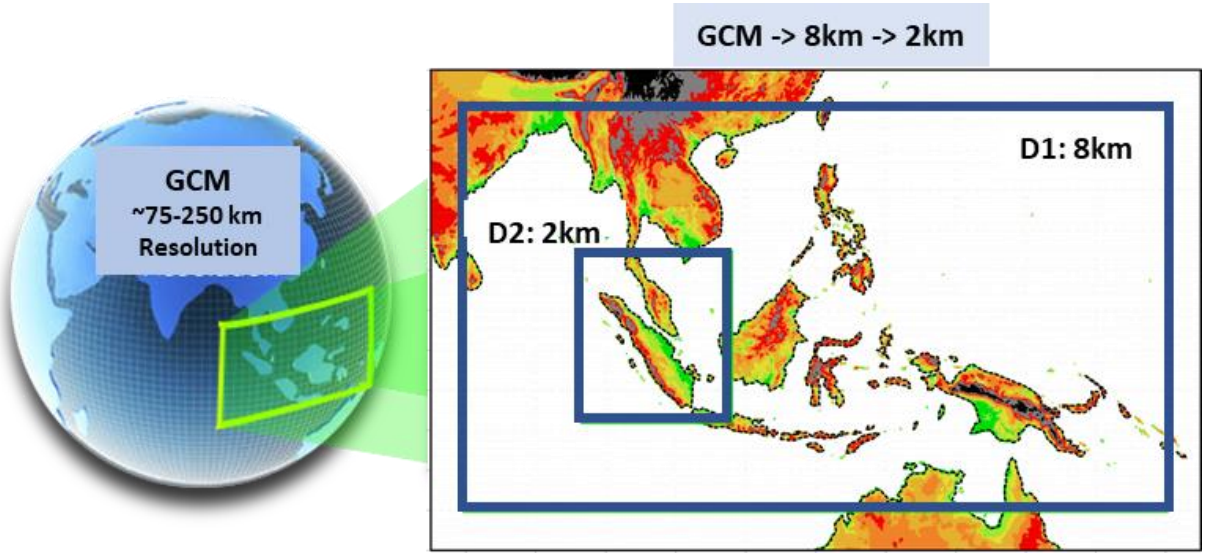

Figure 9.1: The V3 regional climate model domains. 8km resolution simulations are carried out over the D1 domain, and the 2km resolution simulations are carried out over the D2 domain.

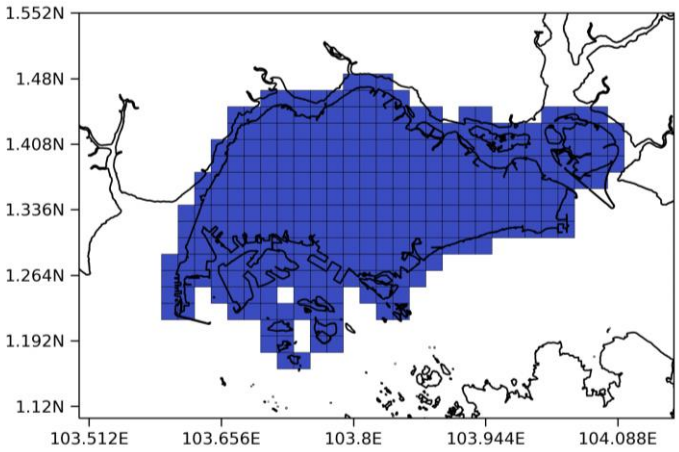

Figure 9.2: Landsea mask for the SG region in the 2km resolution

9.2.3 Variables for bias Adjustments

Here we focus on the following daily variables to carry out the bias adjustment given their relevance to possible future climate impact studies as raised by key stakeholder groups (Table 9.4).

Table 9.4: Variables for bias adjustment

Variable Name	Unit	Description	Relevance to impact studies
pr	mm/day	daily mean of precipitation	plays a crucial role in studying rainfall patterns, droughts, and wet spells
tas	°C	daily mean of near surface air temperature	essential factor in understanding and assessing climate conditions
tasmax	°C	daily maximum of near surface air temperature	providing insights into extreme heat events and temperature extremes
tasmin	°C	daily minimum of near surface air temperature	allowing for the analysis of cold spells and temperature variations
hurs	%	daily mean of near surface relative humidity	contributes to the understanding of moisture levels and atmospheric conditions
sfcWind	m/s	daily mean of 10m wind speed	important for studying wind patterns, gusts, and potential impacts on various sectors

9.2.4 Gridded reference for bias adjustments

To conduct bias adjustments, it is crucial to have gridded observations that cover Singapore and its surrounding area at a daily frequency and in spatial resolutions of 8km and 2km. However, it is challenging to find existing observation products that fully meet these requirements. As a result, additional efforts were undertaken to create suitable benchmark datasets for our study.

Here we employed different approaches for different variables, as outlined in Table 9.5. For precipitation, we utilized station data and applied advanced spatial interpolation methods, specifically Kriging, to generate a gridded precipitation product. This allowed us to convert the point station data into a spatially distributed precipitation dataset, providing a more comprehensive representation of precipitation patterns over Singapore. For the variables of temperature (tas, tasmax, tasmin), relative humidity (hurs), and surface wind speed (sfcWind), we used the ERA5-RCMs as the gridded references. ERA5-RCM is the ERA5-driven regional downscaling simulation using our own SINGV-RCM model (documented in the Chapter 6). By truncating the model outputs for the Singapore domain, we obtained gridded references that align with regional information provided by ERA5 reanalysis but focus on the

spatial extent of Singapore. These ERA5-RCM-based references were found to provide a realistic gridded representation of the selected variables over Singapore, exhibiting good agreement with the point station data across the region.

It is important to note that while efforts were made to create the best available observation benchmarks, observations are not perfect. As new observation products become available in the future, the observation benchmarks can be updated to further improve the accuracy and representativeness of the gridded references.

Table 9.5: Observation references

Resolution	Variable	Source	Period	Additional remarks
2km	pr	krig	1995-2014	using hourly rainfall from 28 stations
8km	pr	krig	1995-2014	using hourly rainfall from 28 stations
2km	tas, tasmax, tasmin, hurs, sfcWind	ERA5-RCM	1995-2014	using 2km daily output from ERA5-driven SINGV-RCM
8km	tas, tasmax, tasmin, hurs, sfcWind	ERA5-RCM	1995-2014	2km daily ERA5-RCM remapped to 8km resolution

9.3 Methods

9.3.1 Bias Adjustment methods

Bias adjustment is a common post-processing technique used in downscaling model applications. One may be aware of two basic “Delta” methods (e.g., Gleick, 1986, Hay et al., 2000). The model-observation “Delta” method calculates the historical model-observation “mean” bias and adds this difference to the future model simulation to correct the “mean” bias in the future projection. The “Delta” method aims to reduce the systematic errors and bring the model closer to the observed reality. The other historical - future “Delta” method calculates the “mean” change in the simulations from the historical to future period, and adds this change to the historical observation. By construction, these “Delta” methods preserve the “mean” future change. They are straightforward approaches and can be useful when more sophisticated bias correction methods are not feasible due to data limitations or computational resources.

Note that the delta method has its limitations. The delta method might not adequately capture biases in extreme events and high percentiles, given that the method assumes the model bias is constant across all quantiles. More advanced statistical methods like quantile mapping (QM) or distribution-based methods may be necessary to address more complex bias patterns and non-stationarities in the climate data. QM-based methods focus on correcting the cumulative distribution functions (CDFs) of climate variables, by acknowledging that the bias can vary across different parts of the distribution. The quantile mapping method corrects biases in both the mean and the shape of the distribution, making it more flexible in addressing complex bias patterns (Maraun, 2016).

The QM method itself has many developments over years and consists of a variety of implementation algorithms. By default, the conventional QM method (Pierce et al., 2015) does not preserve the future change (i.e., delta). The quantile delta mapping (QDM, Cannon et al. 2015) involves identifying the differences in quantiles between the future projections and historical simulations and then applying these delta differences to adjust the entire CDF of the observations. Cannon et al. (2015) discussed and compared several quantile mapping techniques including conventional QM, detrended quantile mapping (DQM), and quantile delta mapping (QDM) in correcting precipitation outputs from GCMs based on a few precipitation extreme indices. The study pointed out that the QDM method shows advantages in its effectiveness of detrending the projection data through multiple quantiles, and capability of dealing with extreme model projections which may be beyond the scope of the historical record by using a superimposing algorithm.

The basic delta method and the quantile mapping methods are both techniques used in statistical and climate modeling, particularly in the context of downscaling and bias correction. The choice between these methods depends on

the specific characteristics of the data and the research objectives. They are often employed to bridge the gap between coarse-scale climate model projections and finer-scale regional or local projections. More extensive review of bias-correction methods can be referred to Maraun (2016).

9.3.2 V3 bias adjustment: ISIMIP3 method

For the V3 study, we specifically sought a trend-preserving method suitable for climate change studies. Various advanced methods have been developed for this purpose, and a comprehensive survey conducted by Casanueva et al. 2020 highlighted several popular bias adjustment methods. The study demonstrated that quantile trend-preserving methods, such as quantile delta mapping (QDM, Cannon et al. 2015), scaled distribution mapping (SDM, Switanek et al. 2017), and the bias adjustment method from the third phase of the Intersectoral Impact Model Intercomparison Project (ISIMIP3, Lange 2019), tend to preserve the raw signals better for different indices and variables considered.

In line with these findings, for the V3 study, we have chosen to adopt the ISIMIP3 bias correction method. This method is designed to preserve the underlying trends and patterns in the data while effectively adjusting for biases, making them well-suited for our climate change analysis and ensuring the reliability and accuracy of our results.

The ISIMIP community has made significant advancements in the development and refinement of bias adjustment methods over the years. Starting from the ISIMIP Fast Track method introduced by Hempel et al. in 2013, they have made subsequent updates in ISIMIP2 (Frieler et al., 2017) and the most recent version, ISIMIP3 (Lange, 2019). These bias adjustment methods have been widely used in the climate impacts modeling community and have shown promising results. Researchers have employed ISIMIP2 in studies such as Peter et al. (2022), and ISIMIP3 has been utilized in the research conducted by Casanueva et al. (2020). These studies demonstrate the practical application and effectiveness of the ISIMIP bias adjustment methods in addressing biases in climate data for various modeling purposes. Furthermore, it is worth noting that the ISIMIP3 scripts are regularly updated to improve their functionality and performance. The updates from Version 1.0 to the current Version 2.5 are publicly available (https://doi.org/10.5281/zenodo.4686991), providing researchers with the most up-to-date tools for implementing bias adjustment in their climate modeling studies. These updates ensure that the bias adjustment methods stay relevant and incorporate the latest advancements in the field. The continuous development and refinement of the ISIMIP bias adjustment methods reflect the commitment of the scientific community to enhance the accuracy and reliability of climate impact assessments and improve our understanding of climate change effects.

One aspect of bias adjustment methods in climate modeling is to handle complex situations and address biases across various time scales and multivariate dependencies. Several studies have proposed advanced methods to handle such complexities and improve the performance of bias correction. For example, Mehrotra and Sharma (2016) developed a method to correct the duration of observed events using an auto-regressive model, which can be particularly useful when simulations fail to capture the realistic duration of events.

Additionally, Mehrotra and Sharma (2012) proposed recursive bias correction methods that can address biases across different time scales, ranging from daily to interannual, allowing for a comprehensive correction approach. In situations where there is a need to account for the multivariate dependence between variables, Cannon (2017) introduced multivariate methods that utilize lagged correlation and regression models. These approaches enable the correction of biases between variables such as precipitation (pr) and temperature (tas) at specific time scales, improving the overall fidelity of the simulation outputs. It's important to note that these advanced methods require sufficient high-quality data to robustly fit the parameters and achieve good performance. Overfitting can be a concern when data availability is limited, as it may lead to artifacts in the bias-corrected outcomes. Striking a balance between correcting biases and avoiding alterations to the fundamental physics represented in the raw simulations is crucial in order to maintain the integrity of the underlying climate models.

In this context, the ISIMIP3 method offers a well-balanced approach. It incorporates physical

considerations while maintaining a reasonable level of complexity that can be adequately fitted to available data. Although it may not completely eliminate biases, ISIMIP3 provides sufficient bias reduction and adjusts future projections closer to the expected future conditions. By adopting the ISIMIP3 method, the V3 study can strike an appropriate balance between reducing biases and preserving the underlying physics of the raw simulations, allowing for more accurate and dependable climate impact assessments. While raw simulations can still offer valuable insights into the "Delta" changes, bias-adjusted simulations are particularly useful for obtaining accurate information regarding the absolute values, variability, and complete distribution of the climate variables. This ensures that the adjusted simulations provide reliable data for conducting climate impact studies.

9.3.3 Bias adjustment configurations

The ISIMIP3 bias adjustment method offers a comprehensive approach to correct biases in various quantiles across the distribution of variables. Compared to basic delta methods, ISIMIP3's quantile mapping approach provides a more detailed and nuanced correction by considering every quantile individually. ISIMIP3 also allows for different fitting options, such as parametric fits or non-parametric fits, to ensure the best possible representation of the observed data. This flexibility enables the method to adapt to different variable characteristics and improve the accuracy of the bias-adjusted simulations. By adopting the configurations suggested by the ISIMIP3 paper (Table 9.6), our study ensures that the bias adjustments are carried out using recommended settings and approaches. This enhances the reliability and consistency of the bias-adjusted simulations for climate impact studies for Singapore.

Table 9.6: Bias adjustment configurations

Variable	Configurations
pr	python bias_adjustment.py --obs-hist=$FILE_OBS_HIST --sim-hist=$FILE_SIM_HIST --sim-fut=$FILE_SIM_PROJ --sim-fut-ba=$FILE_OUTPUT --variable=$VARNAME --halfwin-upper-bound-climatology 0 --lower-bound 0 --lower-threshold .1 --distribution gamma --trend-preservation mixed --adjust-p-values True
hurs	python bias_adjustment.py --obs-hist=$FILE_OBS_HIST --sim-hist=$FILE_SIM_HIST --sim-fut=$FILE_SIM_PROJ --sim-fut-ba=$FILE_OUTPUT --variable=$VARNAME --halfwin-upper-bound-climatology 0 --lower-bound 0 --lower-threshold .01 --upper-bound 100 --upper-threshold 99.99 --distribution beta --trend-preservation bounded --adjust-p-values True
sfcWind	python bias_adjustment.py --obs-hist=$FILE_OBS_HIST --sim-hist=$FILE_SIM_HIST --sim-fut=$FILE_SIM_PROJ --sim-fut-ba=$FILE_OUTPUT --variable=$VARNAME --halfwin-upper-bound-climatology 0 --lower-bound 0 --lower-threshold .01 --distribution weibull --trend-preservation mixed --adjust-p-values True
tas	python bias_adjustment.py --obs-hist=$FILE_OBS_HIST --sim-hist=$FILE_SIM_HIST --sim-fut=$FILE_SIM_PROJ --sim-fut-ba=$FILE_OUTPUT --variable=$VARNAME --halfwin-upper-bound-climatology 0 --distribution normal --trend-preservation additive --detrend True
tasrange	python bias_adjustment.py --obs-hist=$FILE_OBS_HIST --sim-hist=$FILE_SIM_HIST --sim-fut=$FILE_SIM_PROJ --sim-fut-ba=$FILE_OUTPUT --variable=$VARNAME --halfwin-upper-bound-climatology 0 --lower-bound 0 --lower-threshold .01 --distribution rice --trend-preservation mixed --adjust-p-values True
tasskew	python bias_adjustment.py --obs-hist=$FILE_OBS_HIST --sim-hist=$FILE_SIM_HIST --sim-fut=$FILE_SIM_PROJ --sim-fut-ba=$FILE_OUTPUT --variable=$VARNAME --halfwin-upper-bound-climatology 0 --lower-bound 0 --lower-threshold .0001 --upper-bound 1 --upper-threshold .9999 --distribution beta --trend-preservation bounded --adjust-p-values True
tasmin	tasmin = tas - tasskew x tasrange
tasmax	tasmax = tasrange + tasmin

One important aspect of climate change studies is the preservation of the embedded global warming trends in the variables, particularly in temperature (tas). ISIMIP3 takes this into account and ensures that the trend present in the raw simulations is preserved during the bias correction process. This is crucial for capturing the long-term changes in climate variables and their impacts on various sectors.

The 2-step procedure used by ISIMIP3 for bias adjustment of tasmax and tasmin variables ensures that the physical relationship between these variables is maintained during the correction process. In the first step, two intermediate variables, tasrange and tasskew, are derived. The tasrange represents the temperature range and is calculated as the difference between tasmax and tasmin (tasrange = tasmax - tasmin). Tasskew is a measure calculated as the ratio of the difference between tas and tasmin to tasrange (tasskew = (tas - tasmin) / tasrange). In the second step, bias adjustments are applied to tasrange and tasskew. Finally, using the bias-adjusted values of tasrange and tasskew, the bias-adjusted tasmin and tasmax are derived. The tasmin is calculated by subtracting the product of tasskew and tasrange from tas (tasmin = tas - tasskew x tasrange), and tasmax is obtained by adding tasrange to tasmin (tasmax = tasrange + tasmin). By incorporating this additional procedure, the ISIMIP3 method ensures that the physical consistency between tas, tasmax, and tasmin is preserved in the bias-adjusted simulations. This helps to maintain the appropriate temperature relationships and improves the overall realism of the corrected temperature variables.

For precipitation (pr), ISIMIP3 includes specific treatments to address certain issues in the simulations. It implements a lower bound at 0 mm/day to prevent negative (physically unrealistic) precipitation values. Additionally, a lower threshold at 0.1 mm/day is used to correct the drizzle issue commonly observed in simulations, where very low precipitation amounts are overestimated. These treatments improve the realism of the bias-adjusted precipitation simulations.

The bias_adjustment.py script, along with the utility_function.py script, forms the main components for conducting bias adjustment in the ISIMIP3 method. Here's a breakdown of their functionalities: 1. bias_adjustment.py: This script serves as the main function for the bias adjustment process. 2. utility_function.py: This script contains various subroutines and utility functions that support the bias adjustment process. It includes functions for data handling, interpolation, statistical calculations, and other necessary operations. By utilizing these scripts and their functionalities, the bias adjustment process can be carried out effectively and efficiently. The scripts automate the correction procedure for each grid cell or station, ensuring consistency and coherence in the bias-corrected data across space and time.

9.3.4 Combining 2km and 8km resolution bias-adjusted outputs

We conducted bias adjustments for both the 2km and 8km simulations in our study. The 2km simulations provide a detailed spatial pattern over Singapore and the West Maritime Continent, making them suitable for analyzing climate change on a local scale. However, it's important to note that the 2km simulations cover a shorter time period, specifically 1995-2014, 2040-2059, and 2080-2099. To address the long-term trend, we also utilized the 8km bias-corrected simulations, which cover a longer period from 1955 to 2014 for the historical period and from 2015 to 2099 for the future warming period. Although the 8km simulations give a coarser spatial resolution, they provide useful insights into the climate change over a broader time span.

It is worth mentioning that the information and conclusions based on both the 2km and 8km simulations are consistent. We combined the results from both resolutions to address the long-term changes and capture the detailed spatial structure over Singapore. By incorporating strengths of the 2km and 8km simulations, we gained a comprehensive understanding of the climate change trends and their local implications. This approach ensures the robustness of our analysis and enhances the reliability of our findings.

9.3.5 Advances from V2 to V3

In the V2 study, bias adjustment was briefly addressed in Chapter 5 (Climate Change Projections, Annexe 5a: Description of the Quantile Matching technique applied to provide bias-corrected RCM outputs over Singapore). Here we highlight the advances in the V3 bias

adjustment compared to the V2 study (Table 9.7). These advancements have led to more accurate and reliable simulations, providing improved data for climate impact studies over Singapore.

Table 9.7. Advances from V2 to V3 bias adjustment

Advances in V3	V2	V3
higher resolution	V2 study adjusted model output on the 12km resolution over singapore (8 grid cells)	V3 study provided higher resolution bias-adjusted outcome on the 8km (25 grid cells) and 2 km resolution (over 300 grid cells)
new observation reference	V2 used stations across Singapore to aggregate into one CDF as the reference. 3 stations for temperature and humidity, one station for wind, and 28 stations for rainfall. There is no spatial information in the observation reference.	V3 uses ERA5-RCM data to create gridded observational reference for temperature, humidity, and wind. V3 also uses 28 stations to create gridded rainfall reference. These efforts created gridded benchmarks for bias adjustment in the 8km and 2 km resolution.
customised distributions	V2 carried out the same configuration (i.e. multiplicative quantile mapping) to all the target variables.	V3 applied customised configurations for individual variables. e.g., temperature using normal distribution, precipitation using Gamma distribution, relative humidity using beta distribution, and wind using Weibull distribution.
trend-preserving	V2 didn't have treatments for the trend in the historical data and in the model simulations.	V3 has additional treatment to preserve the trend.
adjust rainfall frequency	V2 didn't have treatment for days with zero-rainfall and the low rainfall range.	V3 applies a threshold at 0.1mm/day to adjust the rainfall frequency.
flexible bins for CDF	V2 used 1 percentile bin size to group data in the cumulative distribution function (CDF).	V3 uses the default 0.5 percentile bin size for grouping. But it is adjusted automatically to make sure there are enough samples in each bin to handle zero-rain days.
updated base period	V2 used 1980-2009 30-year as the base period.	V3 uses 1995-2014 20-year as the baseline, which is inline with the IPCC AR6 guidelines.

9.4 Results: bias-adjustment for tas

Historical gridded reference: The evaluation depicted in Figure 9.3 demonstrates a good agreement between the 12-month climatology of the ERA5-RCM and the observed temperature (tas) from five manned stations in Singapore (locations shown in Figure 9.3a). This agreement indicates that the ERA5-RCM simulations can serve as a reasonably realistic gridded reference for temperature (tas) in Singapore for the bias correction process.

Bias-adjusted historical climatology: Figure 9.4 illustrates the historical surface air temperature (tas) over Singapore, showing temperature peaks typically occurring around May. While the models are generally able to capture the seasonal cycle, they tend to overestimate the temperature by approximately 1 degree Celsius. After applying the bias adjustment to the models, the corrected tas align much more closely with the observation reference, indicating a successful correction of the overestimation bias. The bias-adjusted simulations provide a more accurate representation of the observed temperature patterns over Singapore.

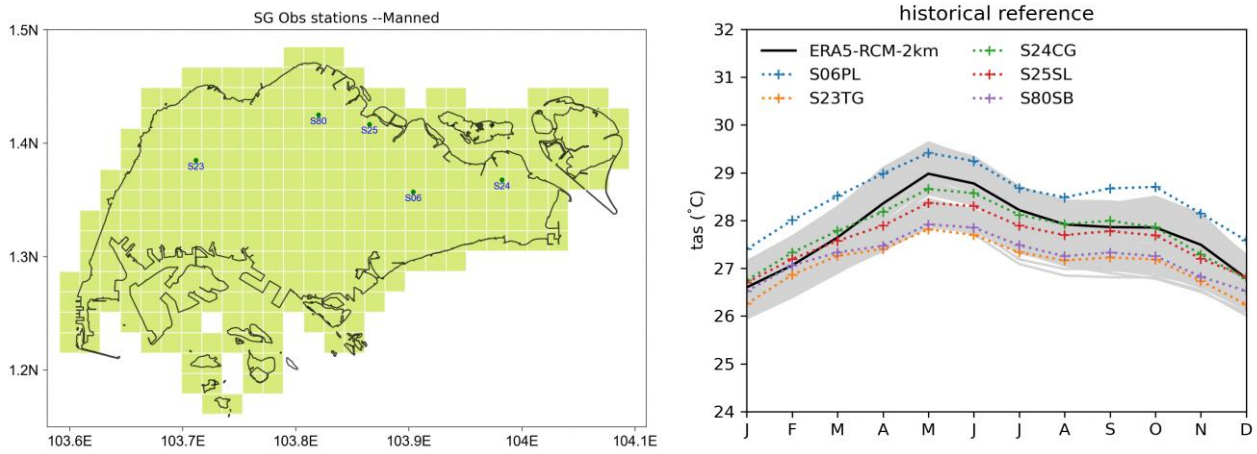

Figure 9.3. (a) map of manned station in Singapore. (b) 12-month climatology of tas in the historical period (1995-2014) from 5 manned stations (dotted) and from 2km-resolution ERA5-RCM gridcells across Singapaore (black is the gridcell mean)

Bias-adjusted future climatology: The models consistently exhibit a tendency to overestimate the surface air temperature by approximately 1 degree Celsius, both in the historical and future periods. After applying the bias adjustment based on the historical reference, the future tas projections are tuned down, bringing them into a more realistic range and better align with expectations based on the observational baseline. This bias adjustment helps to improve the accuracy of the future tas simulations. Figure 9.5 provides visual evidence of this improvement in the bias-adjusted future tas projections.

Future change largely preserved after bias adjustments: Figure 9.6 illustrates the projected changes in surface air temperature (tas) over Singapore. The results indicate a range of warming levels across models, ranging from approximately 2 to 5 degrees Celsius. On average, the models project a mean warming of around 4 degrees Celsius, representing a 15% increase in temperature. It is worth noting that these warming levels are consistent across seasons, indicating a relatively uniform temperature increase throughout the year.
The comparison between the bias-adjusted simulations and the original projections demonstrates that the warming signals are largely preserved after the bias adjustment process. This indicates that the adjustments successfully correct the systematic biases without significantly altering the projected changes in tas. The preserved warming signals in the bias-adjusted simulations provide a more reliable representation of the expected future climate conditions over Singapore.

Climate change patterns largely preserved by bias adjustments: Figure 9.7 illustrates the spatial pattern of projected warming signals across Singapore for both raw and bias-adjusted simulations from the UKESM1-0-LL model. It is evident that there are spatial differences in the projected warming, with northern Singapore exhibiting a larger warming signal compared to the southern parts of Singapore, which are closer to the open ocean.

The bias adjustment process aims to preserve the spatial features of the warming signals while reducing systematic biases in the model simulations. The comparison for UKESM1-0-LL shows that both raw and bias-adjusted simulations keep consistency in the magnitude of the warming signal. Furthermore, the bias adjustment successfully preserves the spatial differences in the warming patterns. The larger warming signal observed in northern Singapore, as seen in the raw simulations, is also maintained in the bias-adjusted simulations.

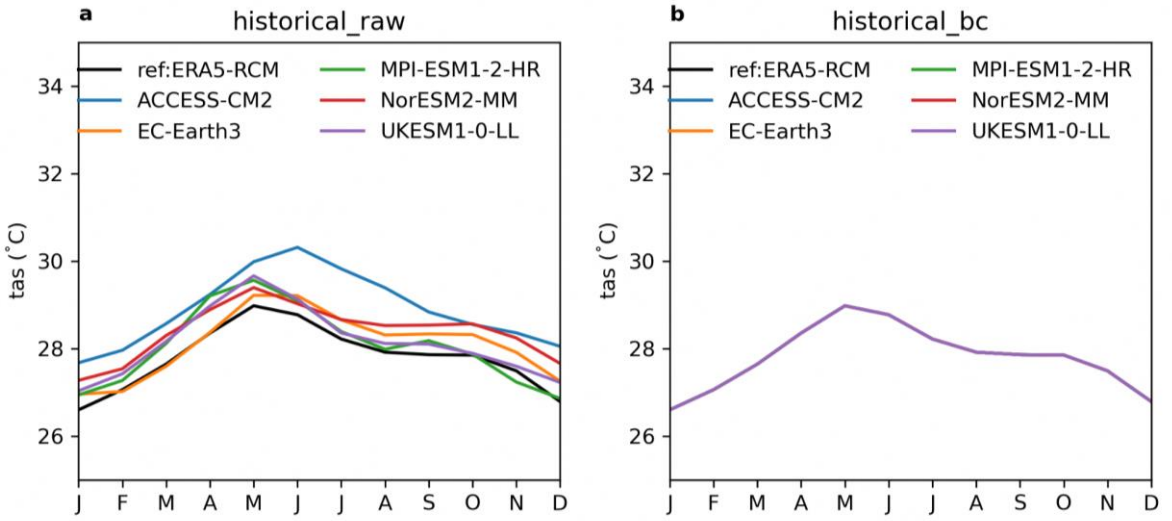

Figure 9.4: Singapore domain-averaged tas at the 2km resolution in the historical period (1995-2014). a. observation reference (ERA5-RCM) and raw simulations. b. similar to a, but plotting bias-adjusted simulations.

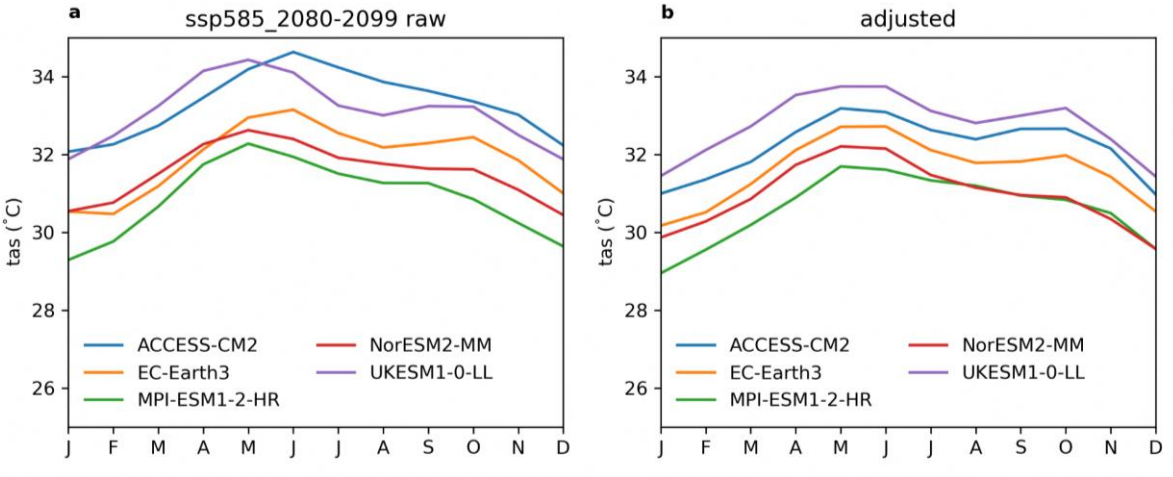

Figure 9.5: Singapore domain-averaged tas in the SSP585 future period (2080-2099) at the 2km resolution. a. raw simulations. b. bias-adjusted simulations.

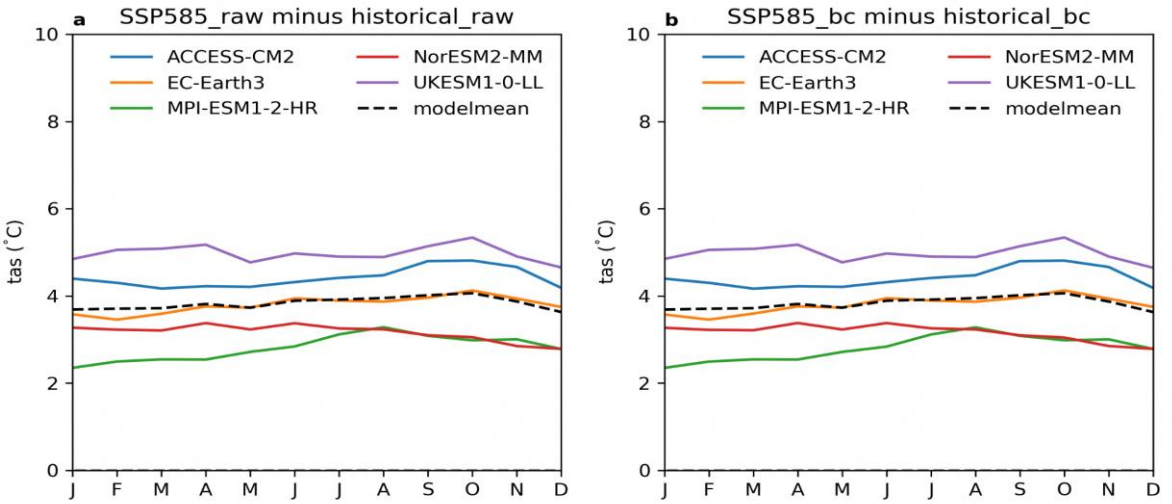

Figure 9.6: Changes in the Singapore domain-averaged tas from the historical period (1995-2014) to the future period (2080-2099) under the SSP585 scenario at the 2km resolution. a. raw simulations. b. bias-adjusted simulations.

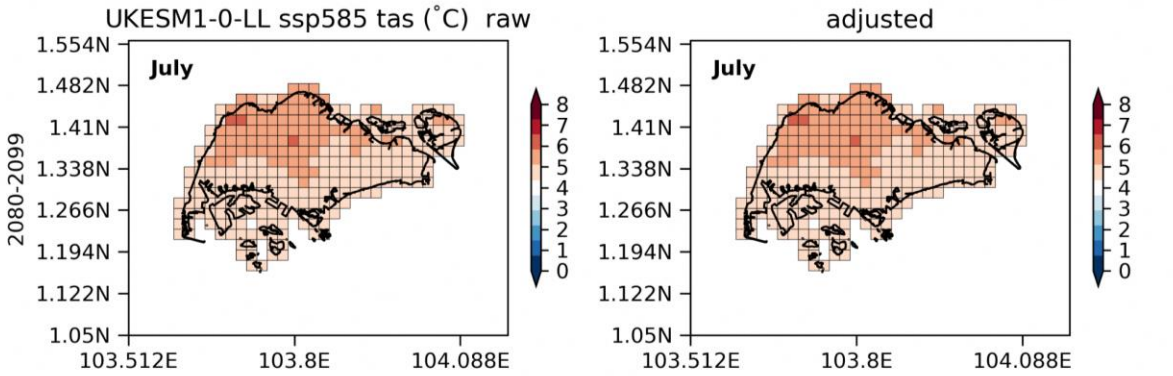

Figure 9.7: 2km resolution Singapore tas change in July from the historical period to the future period under the SSP585 scenario in the UKESM1-0-LL. a. raw simulations. b. bias-adjusted simulations.

Bias-adjusted distribution: Figure 9.8 presents the distributions of daily tas (surface air temperature) for both raw and bias-adjusted simulations from individual models, along with the reference distribution from ERA5-RCM. It is shown that the overall distribution of daily tas follows a normal distribution.

The bias adjustment process successfully brings the model simulations into better agreement with the observed distribution. Furthermore, when considering the effect of warming on tas, models that initially overestimate the warming are tuned down during the bias adjustment process. This can be observed in Figure 9.8b. This downshifted distribution reflects the adjustment made to bring the models' projected warming to a more realistic range. Overall, the bias adjustment method ensures that the bias-adjusted simulations provide a more accurate representation of the expected distribution of daily tas, considering both historical observations and projected future changes.

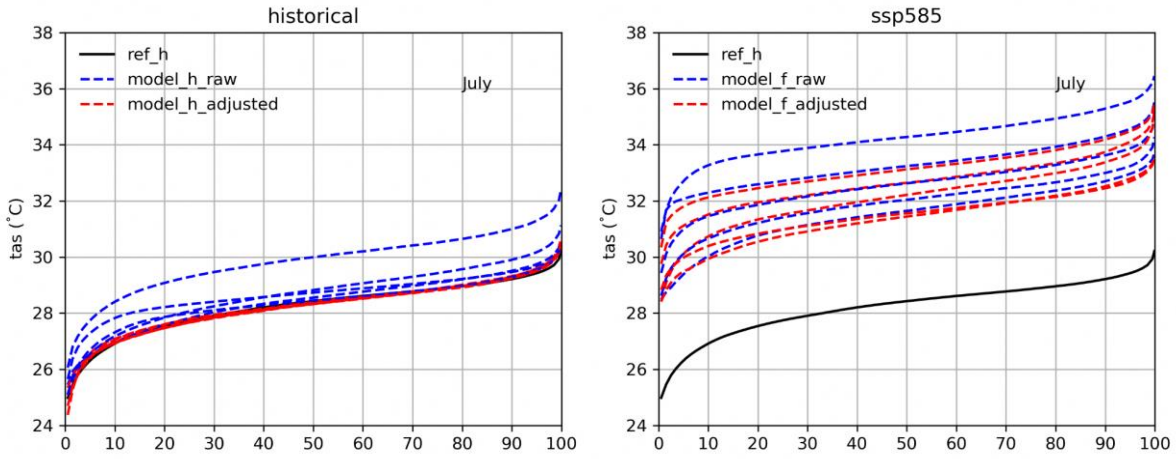

Figure 9.8: (a) July CDF of tas at gridcells across Singapore for the historical period (1995-2014). Here the ref_h is ERA5-RCM, model_h_raw are raw simulations, and model_h_adjusted are adjusted models. (b) July CDF for the future period (2080-2099) under the SSP585 scenario.

Trend in annual mean tas: Figure 9.9 highlights the climate change signal in tas (surface air temperature) and the performance of the bias-adjusted simulations in capturing this signal. It demonstrates that the bias-adjusted tas successfully preserves the warming trend associated with climate change.

In the historical period, the time series of tas in the models are adjusted to match the mean of the observed data. This adjustment ensures that the model simulations are consistent with the observed mean temperature, providing a more accurate representation of historical climate conditions. Furthermore, the variability range of the adjusted simulations in the historical period is similar to that of the observations. This suggests that the bias adjustment process not only corrects for biases in the mean tas but also addresses discrepancies in the variability, allowing the adjusted simulations to capture the observed range of temperature variations.

Looking into the future period, the bias-adjusted time series provide a more realistic projection of tas. The adjusted simulations not only capture the adjusted mean temperature but also maintain a realistic range of variability. Overall, the bias-adjusted tas preserves the important climate change signal by capturing the warming trend and matches the mean and variability of the observations in the historical period. In the future period, the adjusted simulations offer a more realistic projection of tas, ensuring that the bias adjustment process enhances the accuracy and reliability of the model outputs.

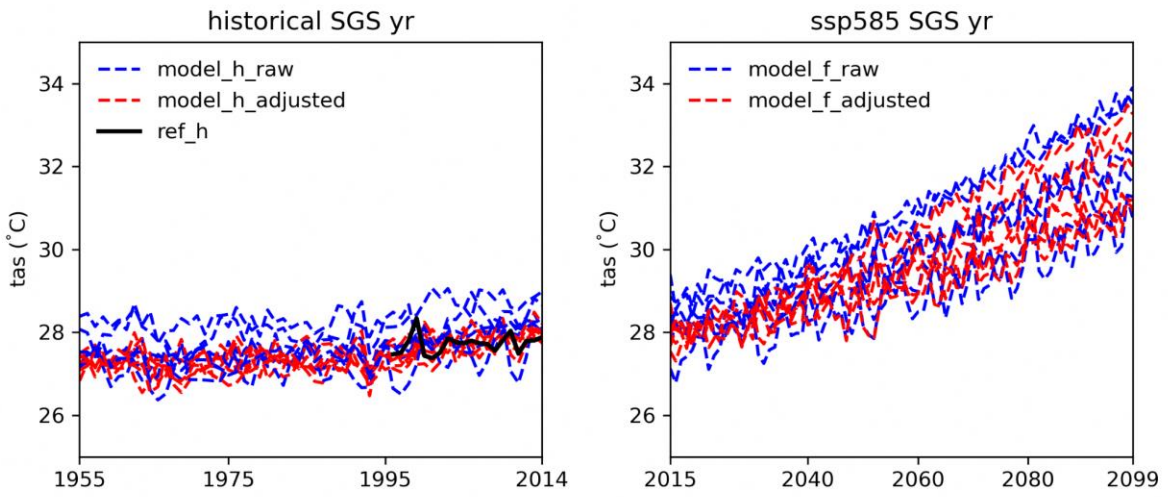

Figure 9.9: (a) 8km resolution Singapore domain-averaged tas in the historical period. (b) tas in the future period under the SSP585 scenario. Observation reference is in black (ERA5-RCM). Raw simulations are in blue, and bias-adjusted simulations are in red.

9.5 Results: bias-adjustment for tasmax

Historical gridded reference: Here we use ERA5-RCM as the historical reference. Comparison showed that the 12-month climatology of tasmax observations from 5 manned stations in Singapore are within the range of the climatology of tasmax at each gridcells from the ERA5-RCM (Figure 9.10). It indicates that ERA5-RCM can provide a reasonably realistic gridded reference for tasmax.

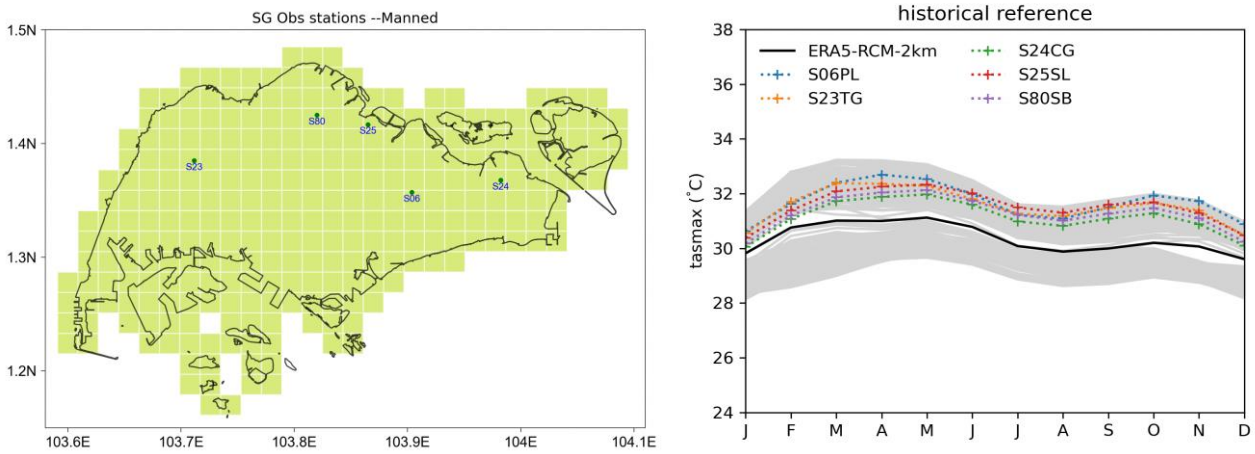

Figure 9.10. (a) Map of manned stations in Singapore. (b) 12-month climatology of tasmax from 5 manned stations (dotted) and from ERA5-RCM gridcells across Singapaore (black is the gridcell mean).

Bias-adjusted historical climatology: Historical tasmax over Singapore shows temperature peaks around March-April-May (Figure 9.11). Models are able to simulate the seasonal cycle but tend to overestimate the tas for ~1°C. Bias-adjusted simulations match with the observation reference (Figure 9.11).

Bias-adjusted future climatology: Models tend to overestimate the temperature in both historical and future period. Adjusted tasmax is tuned down to provide a more realistic future projection (Figure 9.12).

Climate change signal preserved by bias adjustments: As to the change, models project warming ranging from ~2.5 to ~5.5°C (Figure 9.13) with the mean around 4°C (~13% increase). The warming levels are similar across seasons. Bias adjustments largely preserve the warming.

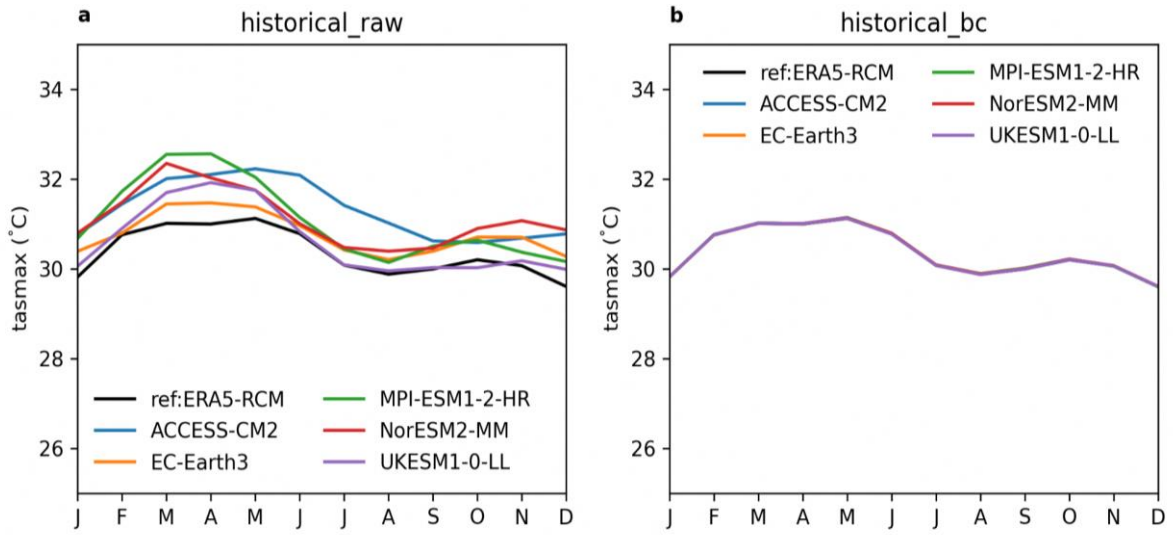

Figure 9.11: Singapore domain-averaged tasmax in the historical period (1995-2014). (a) observation reference (ERA5-RCM) and raw simulations. (b) similar to a, but plotting bias-adjusted simulations.

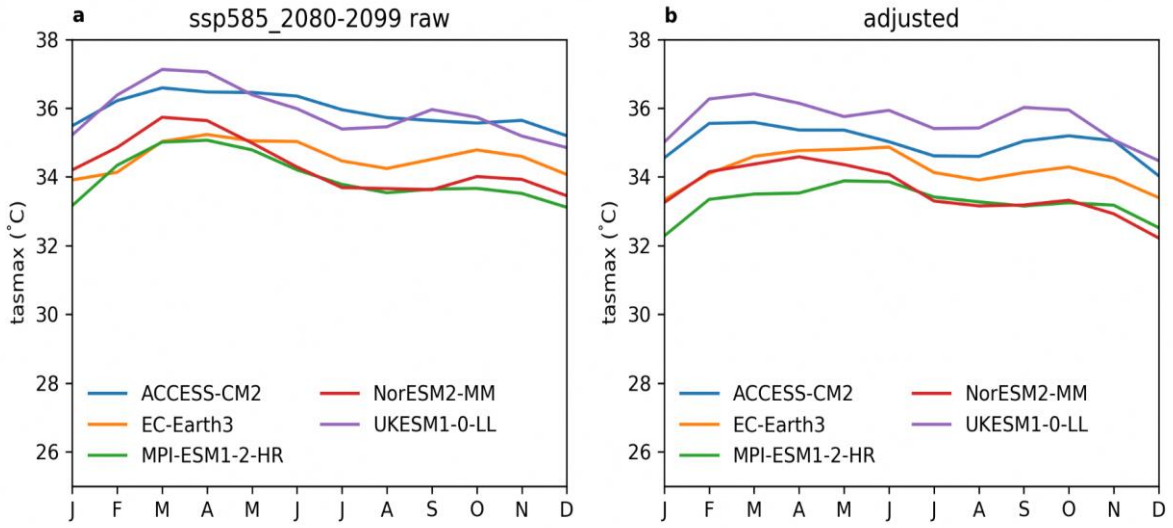

Figure 9.12: Singapore domain-averaged tasmax in the SSP585 future period (2080-2099) at a 2km resolution. a. raw simulations. b. bias-adjusted simulations.

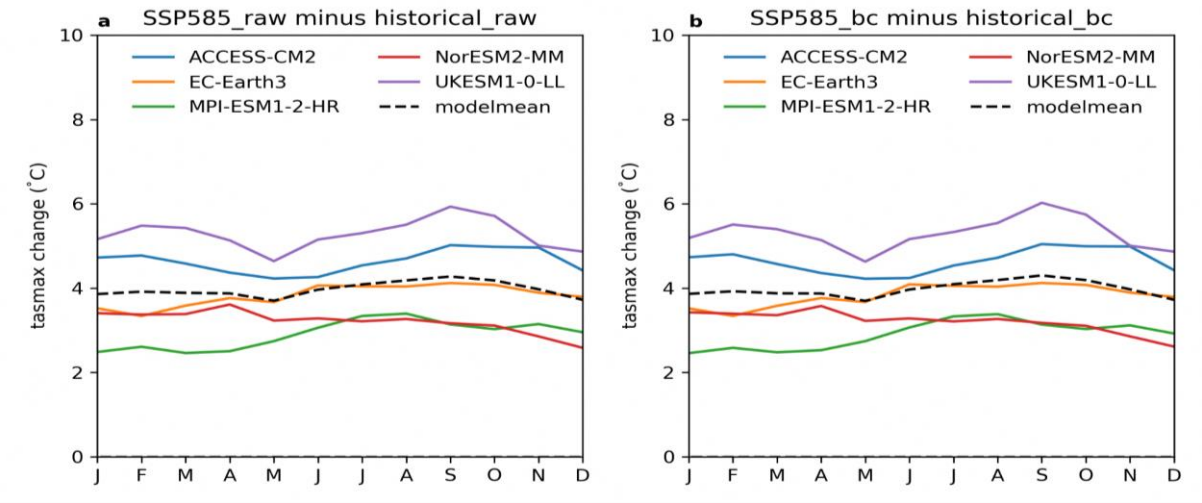

Figure 9.13: Changes in the Singapore domain-averaged tasmax from the historical period (1995-2014) to the future period (2080-2099) under the SSP585 scenario. a. raw simulations. b. bias-adjusted simulations.

Climate change patterns preserved by bias adjustments: Similar to the warming pattern of tas, future change of tasmax in both raw and adjusted simulations show a larger warming in the northern Singapore compared to the southern Singapore (Figure 9.14).

Bias-adjusted distribution: Distributions of modelled tasmax are adjusted to the reference distribution (ERA5-RCM) for the historical period (Figure 9.15). Under warming, distributions of tasmax are tuned down slightly.

Trend in annual mean tasmax: Here we show time series of tasmax in models are adjusted to match observation mean in the historical period (Figure 9.16). Also the variability range of the adjusted simulations is similar to the observation. In the future period, adjusted time series provide more realistic projection with adjusted mean and variability. Here bias adjustment preserved the warming trend in tasmax.

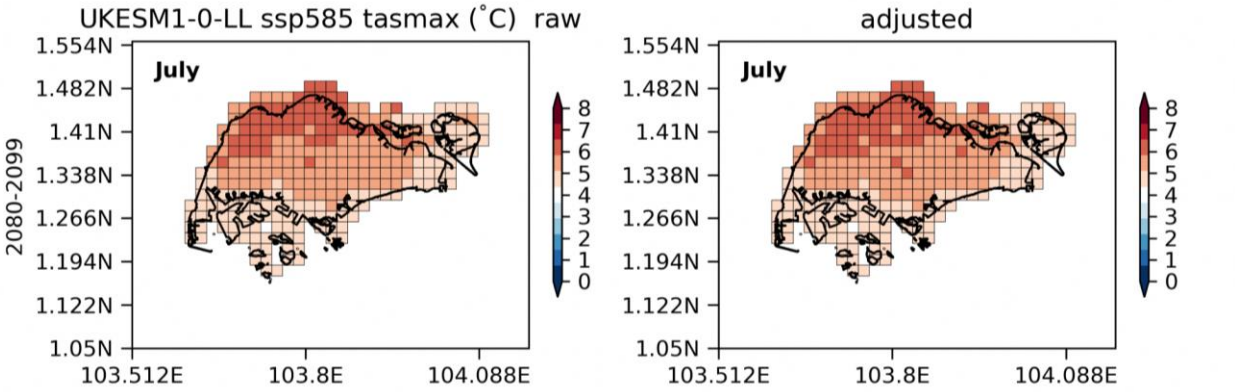

Figure 9.14: 2km resolution Singapore tas change in July from the historical period to the future period under the SSP585 scenario. a. raw simulations. b. bias-adjusted simulations.

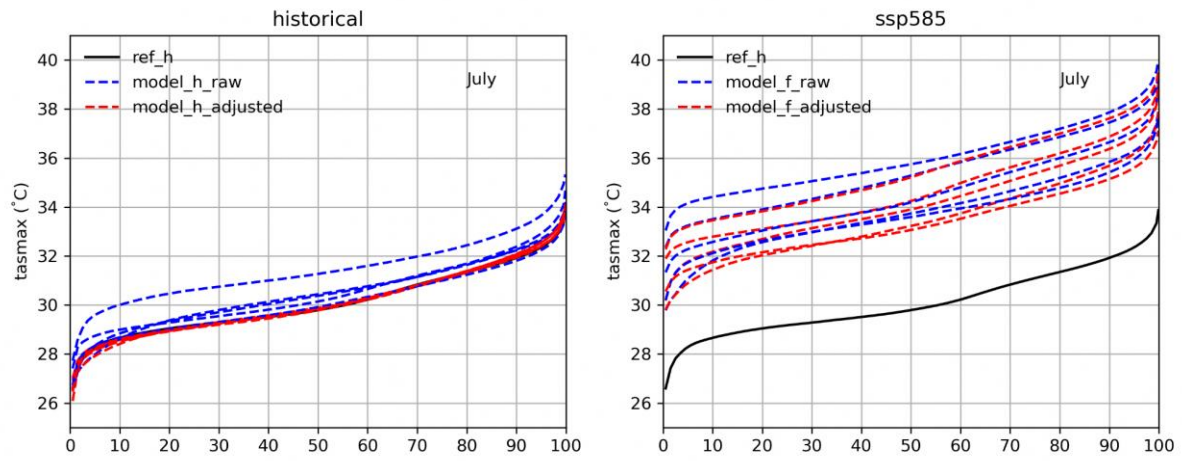

Figure 9.15: a. July CDF of tasmax at gridcells across Singapore for the historical period (1995-2014). Reference is the ERA5-RCM. b. July CDF for the future period (2080-2099) under the SSP585 scenario.

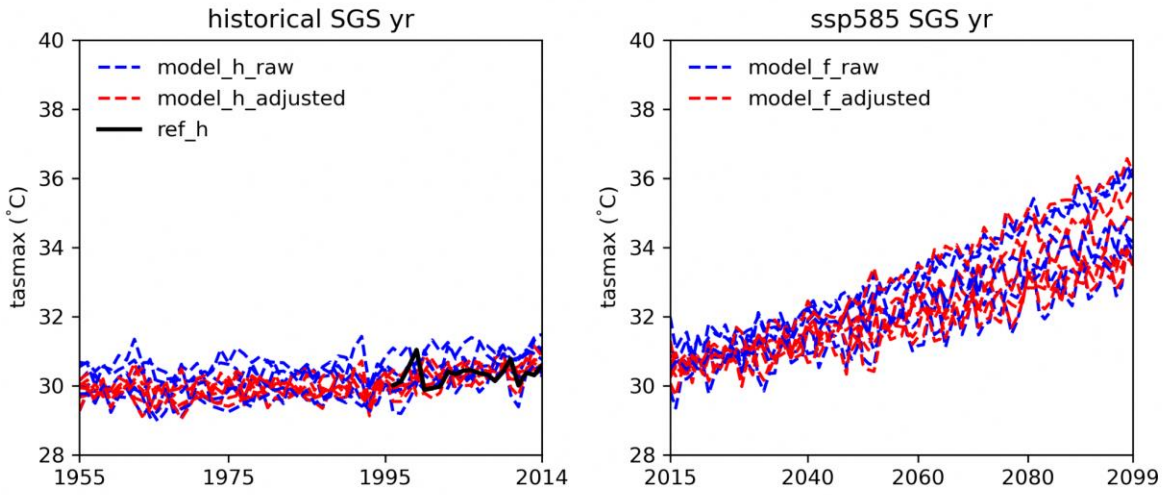

Figure 9.16: 8km resolution Singapore domain-averaged tasmax in the historical period (a) and in the future period (b) under the SSP585 scenario. Observation reference (ERA5-RCM) is in black. Raw simulations are in blue, and bias-adjusted simulations are in red.

9.6 Results: bias-adjustment for tasmin

Historical gridded reference: Here we use ERA5-RCM as the historical reference. We compared the 12-month climatology of the ERA5-RCM with tasmin observations from 5 manned stations in Singapore, and the results (Figure 9.17) show that ERA5-RCM can provide a reasonably realistic gridded reference.

Bias-adjusted historical climatology: The models exhibit similar overestimated biases for tasmin. After applying bias-adjustment techniques, the simulations better align with the observational reference, as shown in Figure 9.18.

Bias-adjusted future climatology: Models tend to slightly overestimate the tasmin in both historical and future period. Adjusted tasmin is tuned down to provide a more realistic future projection (Figure 9.19).

Climate change preserved by bias adjustments: As to the change of tasmin (Figure 9.20), models project warming ranging from ~2 to ~5°C with the mean warming around 4°C (~15% increase). The warming levels are similar across seasons. Bias adjustment can preserve the change signal.

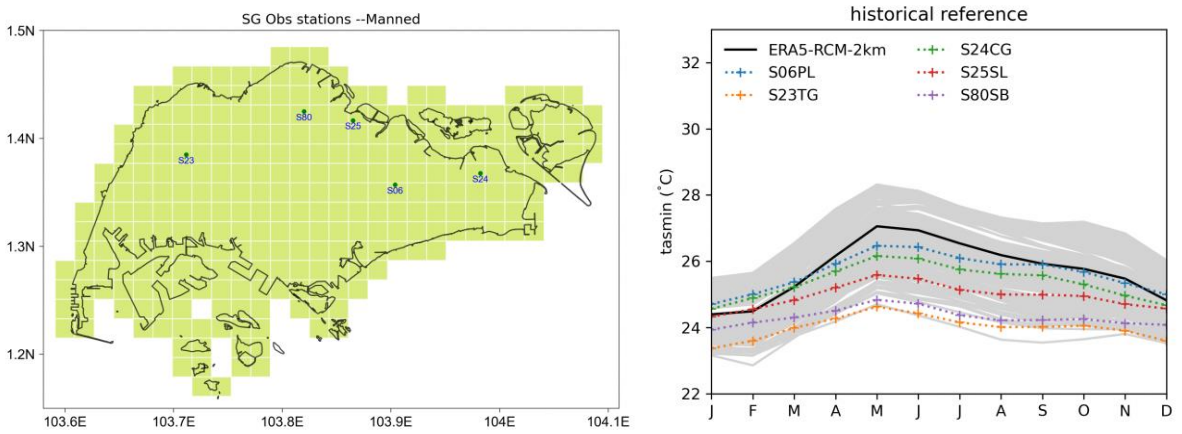

Figure 9.17. a. Map of manned stations in Singapore. b. 12-month climatology of tasmin in the historical period (1995-2014) from 5 manned stations (dotted) and from ERA5-RCM gridcells across Singapaore (black is the gridcell mean).

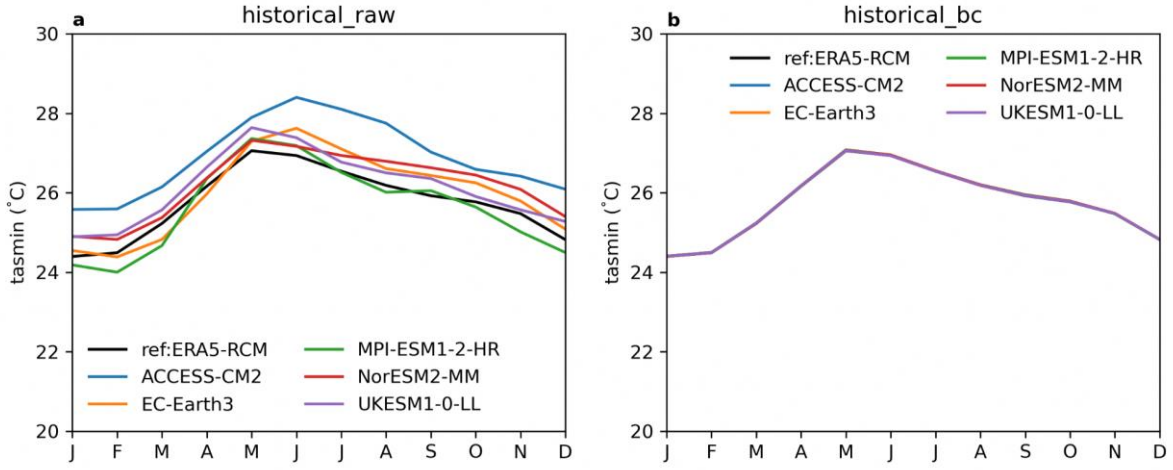

Figure 9.18: Singapore domain-averaged tasmin in the historical period (1995-2014) at a 2km resolution. a. observation reference (ERA5-RCM) and raw simulations. b. similar to a, but plotting bias-adjusted simulations.

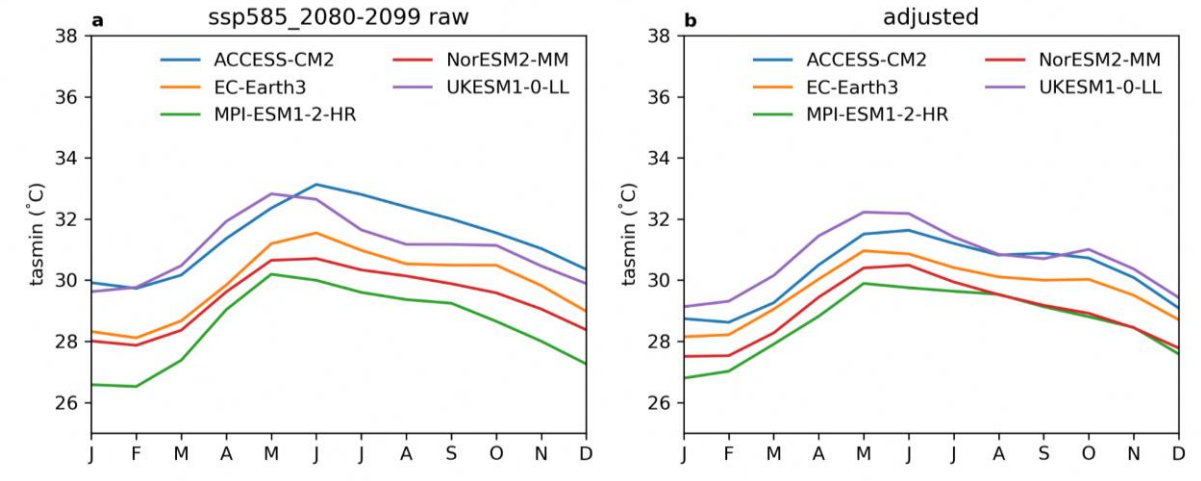

Figure 9.19: Singapore domain-averaged tasmin in the future period (2080-2099) under the SSP585 scenario at a 2km resolution. a. raw simulations. b. bias-adjusted simulations.

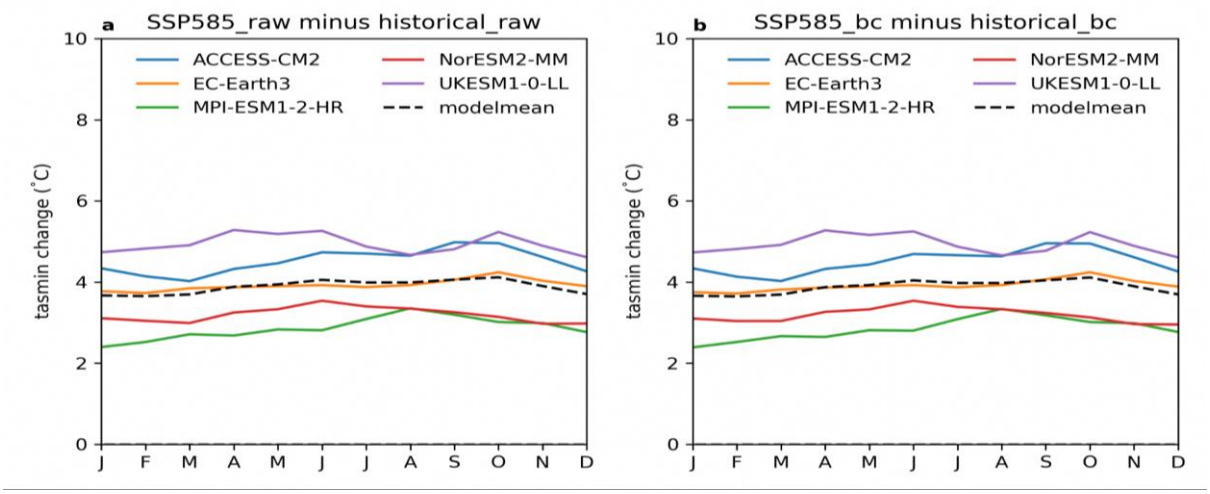

Figure 9.20: Changes in the Singapore domain-averaged tasmin from the historical period (1995-2014) to the future period (2080-2099) under the SSP585 scenario at a 2km resolution. a. raw simulations. b. bias-adjusted simulations.

Climate change patterns preserved by bias adjustments: Similar to the warming pattern of tas, future change of tasmin (Figure 9.21) in both raw and adjusted simulations show a larger warming in the northern Singapore compared to the southern Singapore.

Bias-adjusted distribution: Distributions of modeled tasmin are adjusted to the reference distribution (ERA5-RCM) for the historical period (Figure 9.22). Under warming, distributions of tasmin are tuned down to a more reasonable range of warming.

Trend in annual mean tasmin: Here we show time series of tasmin in models are adjusted to match observation mean in the historical period (Figure 9.23). Also the variability range of the adjusted simulations is similar to the observation. In the future period, adjusted time series provide more realistic projection with adjusted mean and variability. Bias adjustment preserves the warming trend.

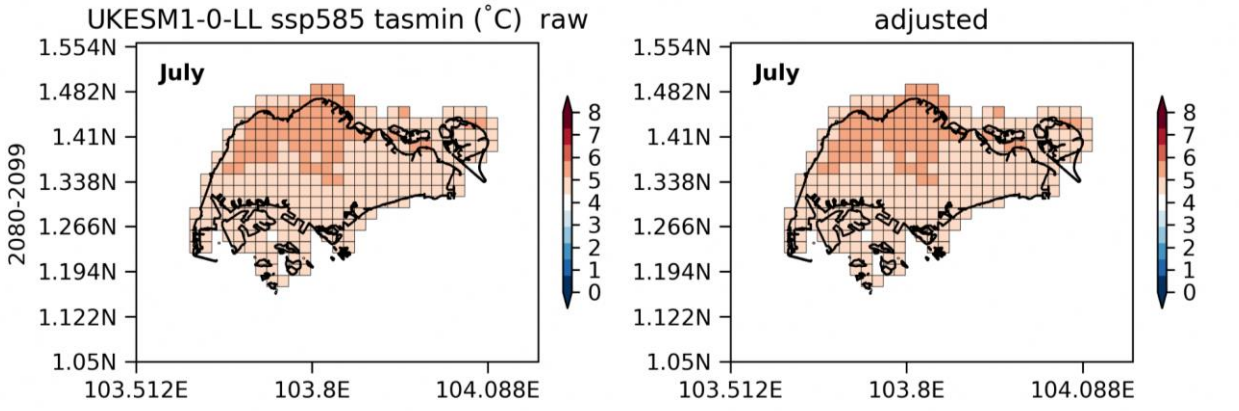

Figure 9.21: 2km resolution Singapore tasmin change in July from the historical period (1995-2014) to the future period (2080-2099) under the SSP585 scenario simulated by UKESM1-0-LL. a. raw simulations. b. bias-adjusted simulations.

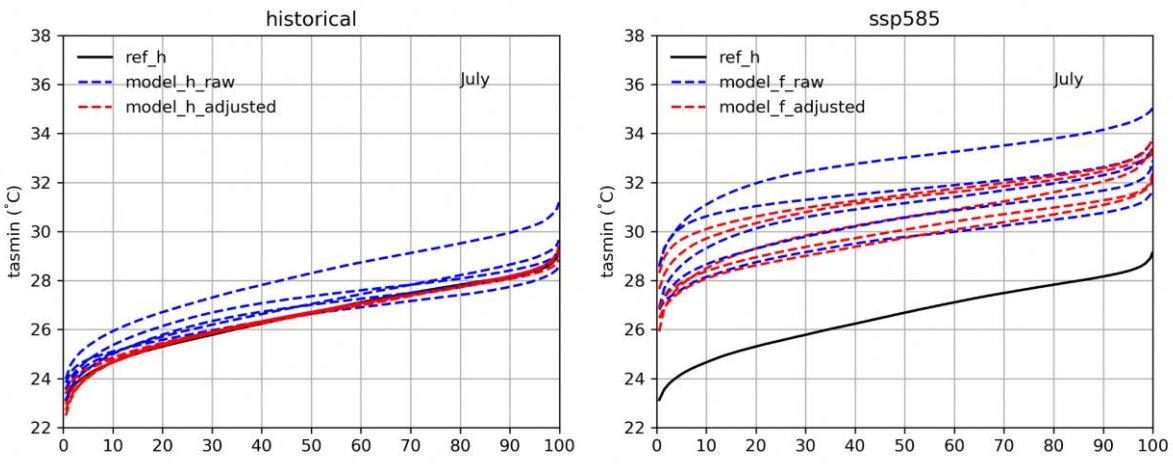

Figure 9.22: a. July CDF of tasmin at gridcells across Singapore for the historical period (1995-2014). b. July CDF for the future period (2080-2099) under the SSP585 scenario.

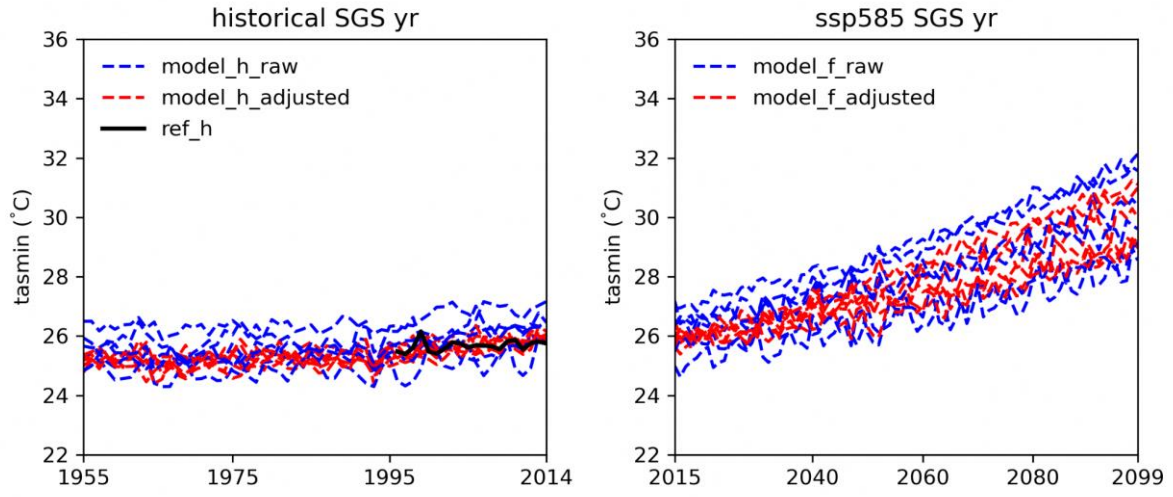

Figure 9.23: a. 8km resolution Singapore domain-averaged tasmin in the historical period. b. tasmin in the future period under the SSP585 scenario. Observation reference is in black (ERA5-RCM). Raw simulations are in blue, and bias-adjusted simulations are in red.

9.7 Results: bias-adjustment for pr

Historical gridded reference: The Meteorological Service Singapore (MSS) has established a network of 93 automatic weather stations (AWS) across Singapore since 2009. However, for long-term rainfall records, there are only around 28 rain-gauge stations available dating back to 1980. Figure 9.24 illustrates the locations of these rain gauges, revealing a limited spatial coverage particularly in western and eastern Singapore.

To overcome this spatial limitation, a gridded daily rainfall dataset was created using geostatistical interpolation techniques. The Python package PyKrige, as described by Murphy et al. (2020), was utilized for this purpose. The interpolation was performed on daily rainfall data aggregated from the hourly data collected at each station. Only days with at least one non-zero rainfall value were considered, while days with no rainfall were assigned a zero value. The geostatistical interpolation employed the concept of Ordinary Kriging, which is a spatial interpolation method based on variograms. A spherical semivariogram model was chosen to capture the spatial autocorrelation and variability of rainfall as a function of the separation distance between each pair of stations. The selection of the spherical model was based on the work of

Muhammad Ali and Othman (2017), who evaluated various semivariogram models and found the spherical model to be the most appropriate for the Kelang River basin in Peninsular Malaysia. By applying geostatistical interpolation using PyKrige and the spherical semivariogram model, the gridded daily rainfall dataset was generated, providing a more comprehensive representation of rainfall across Singapore. This dataset helps address the limited spatial coverage of rain-gauge stations and allows for a more accurate analysis and understanding of rainfall patterns and variability in the region.

The daily rainfall observations from 1980 to 2021 were subjected to spatial interpolation using kriging techniques, specifically applied to the SINGV-RCM 2-km and 8-km grid. This interpolation process resulted in a gridded representation of rainfall station data. For this study, the kriged rainfall observations for the period 1995-2014 were chosen as the reference dataset.

Comparisons between the kriged rainfall and individual rain gauges revealed good agreement in terms of climatological patterns. This agreement suggests that the kriged precipitation data can serve as a suitable gridded observation reference. By utilizing kriging interpolation, the study was able to fill in spatial gaps and provide a more comprehensive representation of rainfall across the region. Using the kriged rainfall observations as the reference, the study can effectively assess and analyze the model performance in capturing the spatial and temporal characteristics of precipitation.

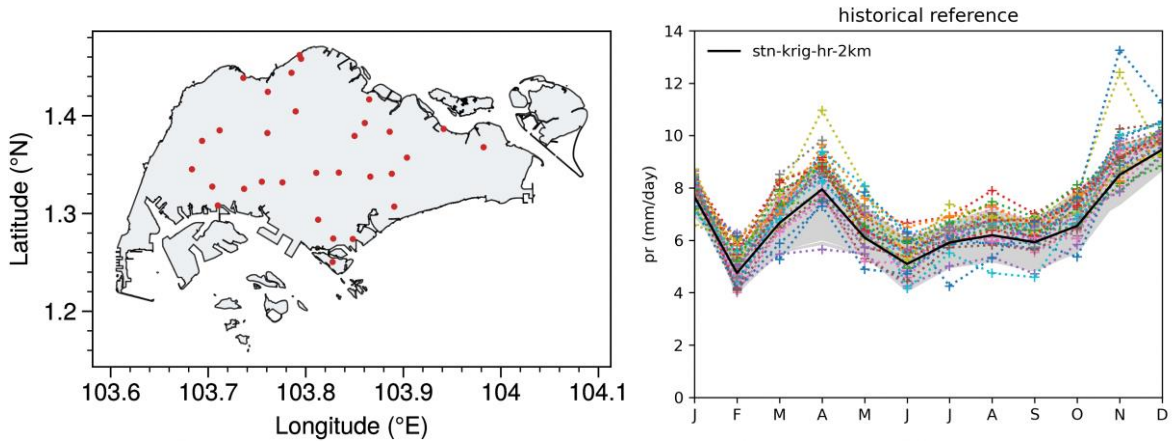

Figure 9.24: a. Map of 28 rain gauge stations in Singapore. b. 12-month climatology of pr in the historical period (1995-2014) from 28 pr stations (dotted) and from 2km-resolution krig gridcells across Singapore (black is the gridcell mean).

Bias-adjusted historical climatology: Historical rainfall over Singapore shows a seasonal transition between weather types (Figure 9.25). It starts from a wet winter due to the Northeast monsoon, followed by another wet April due to frequent squalls moving across Singapore. Then comes the dry summer and autumn due to Southwest monsoon. Here five SINGV RCM models show varying wet/dry biases compared to the observation reference. In particular, models appear to underestimate the January-March rainfall. Bias-adjusted simulations match closely with the reference (Figure 9.25).

Bias-adjusted future climatology: Here we show that (Figure 9.26) raw future rainfall is also low in Jan-Feb (systematic bias, similar to the historical rainfall, see Figure 9.25). After bias-adjustment, the Jan-Feb rainfall is more close to the magnitude of the observation reference.

Climate change overall preserved by bias adjustments: After bias adjustments, models tend to agree that SG may become drier (-3mm/day) by 25% (Figure 9.27) in Jan-Feb and July-Sept, while wetter (+2mm/day) by 20% in May and Nov-Dec. One may notice that the future rainfall changes are tuned down slightly after bias adjustments, unlike the changes in the surface air temperature. It is heavily due to the nonlinearity and skewed distribution in rainfall (Figure 9.29) compared to the relatively normal distribution in temperature (Figure 9.8). For

temperature, the biases are mainly in the mean instead of the shape of the distribution. However, the biases in rainfall are embedded in the whole distribution.

In the process of recalibrating historical and projected precipitation within these skewed distributions, the overall direction of change remains largely intact. However, there is potential for a minor adjustment in the magnitude of mean future changes. It is crucial to also recognize that raw future changes, when derived from biased simulations, do not inherently represent accurate projections. Consequently, changes after the bias adjustments could lead to alterations that are more aligned with realistic expectations. This bias adjustment practice does not alter the understanding and main conclusions as to the future changes.

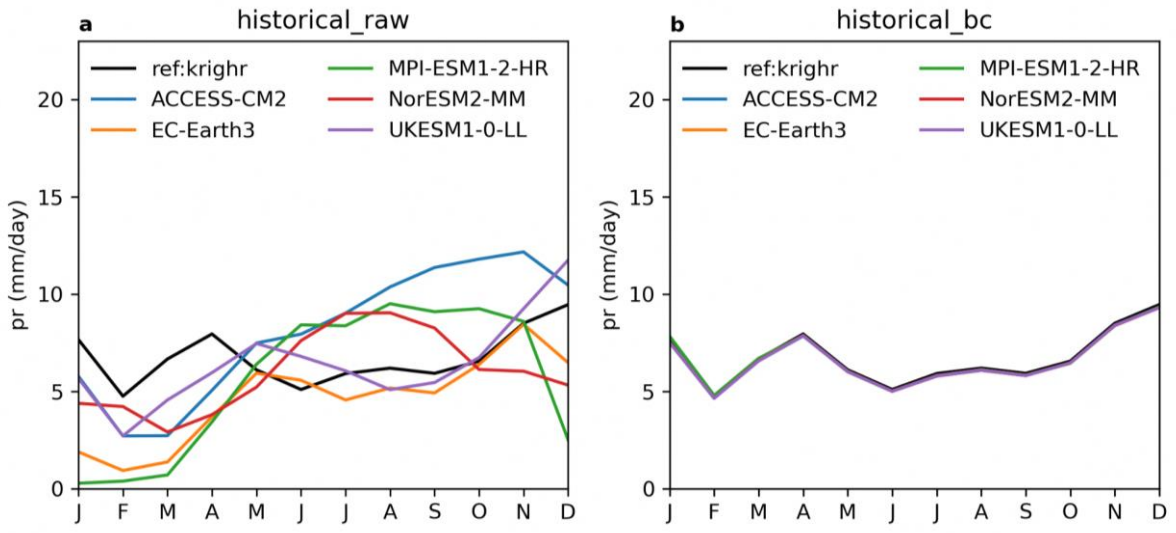

Figure 9.25: Singapore domain-averaged pr in the historical period (1995-2014) at a 2km resolution. a. observation reference (station krig pr) and raw simulations. b. similar to a, but plotting bias-adjusted simulations.

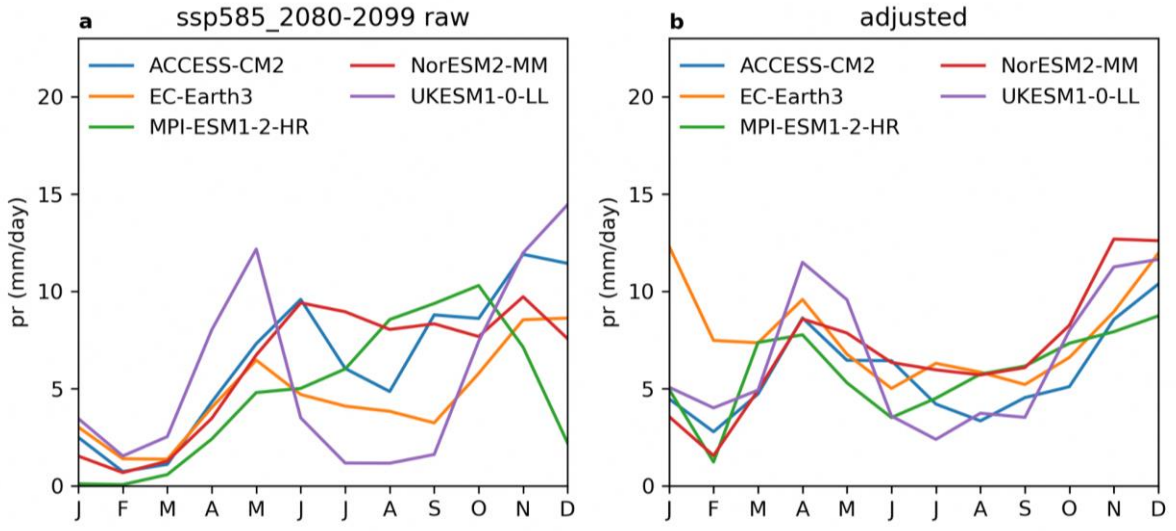

Figure 9.26: Singapore domain-averaged pr in the future period (2080-2099) under the SSP585 scenario. a. raw simulations. b. bias-adjusted simulations.

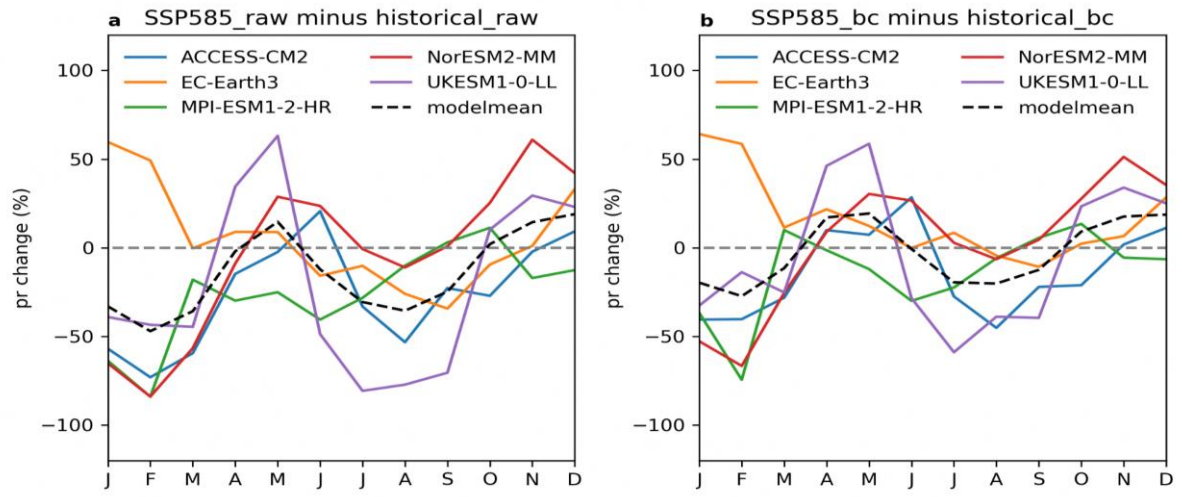

Figure 9.27: Percentage changes in the Singapore domain-averaged pr from the historical period (1995-2014) to the future period (2080-2099) under the SSP585 scenario at a 2km resolution. a. raw simulations. b. bias-adjusted simulations.

Climate change patterns preserved by bias adjustments: Singapore is controlled by southwest monsoon duing the JJAS season. Here future changes in pr projected by ACCESS-CM2 (Figure 9.28) in both raw and adjusted simulations show a larger reduction of rainfall in the south-western Singapore compared to the north-eastern Singapore. Note that bias adjustment still preserve the spatial feature of the change even though the change magnitude is reduced after bias adjustment.

Bias-adjusted distribution: Distributions of modeled pr (overestimated as to the reference) are adjusted to the reference distribution (station kriged) for the historical period (Figure 9.29). Under warming, distributions of overestimated July pr are tuned down.

Trend in annual mean pr: Here we show time series of rainfall in models are adjusted to match observation mean in the historical period (Figure 9.30). Also the variability range of the simulations is reduced to match the observation. In the future period, adjusted time series provide more realistic projection with adjusted mean and variability.

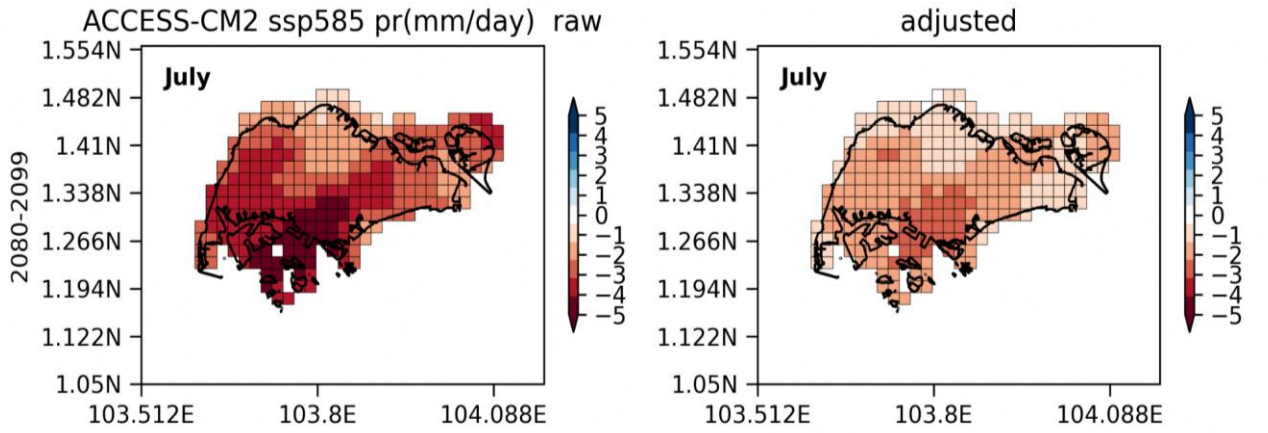

Figure 9.28: 2km resolution Singapore pr change in July from the historical period (1995-2014) to the future period (2080-2099) under the SSP585 scenario. a. raw simulations. b. bias-adjusted simulations.

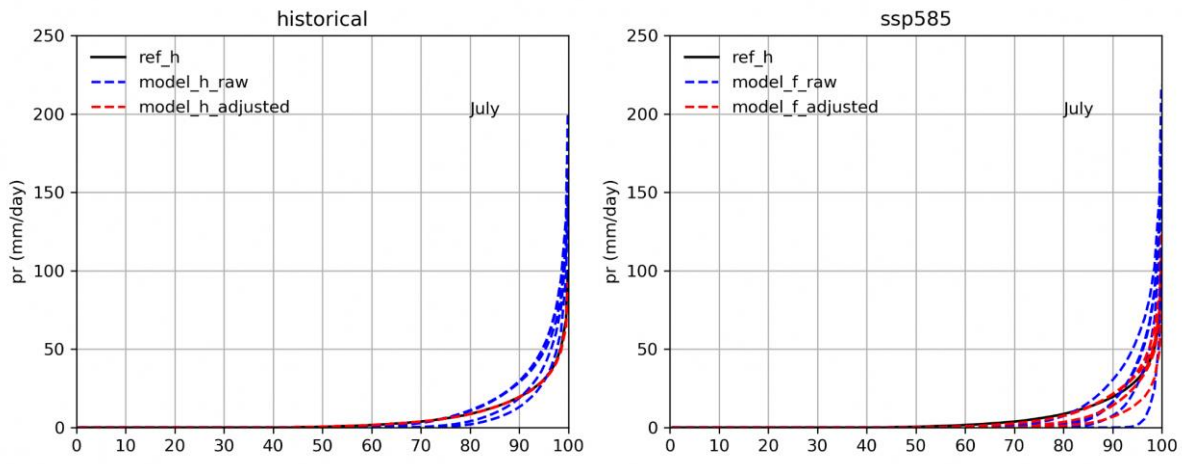

Figure 9.29: a. July CDF of pr at 2km resolution gridcells across Singapore for the historical period (1995-2014). b. July CDF for the future period (2080-2099) under the SSP585 scenario.

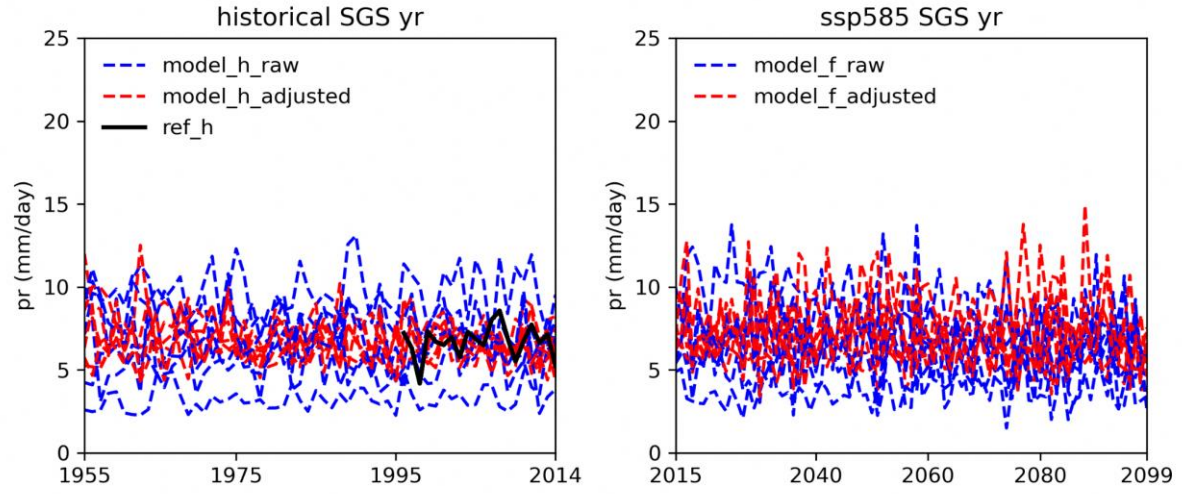

Figure 9.30: a. 8km resolution Singapore domain-averaged annual mean pr in the historical period. b. pr in the future period under the SSP585 scenario. Observation reference is in black (station krig pr). Raw simulations are in blue, and bias-adjusted simulations are in red.

9.8 Results: bias-adjustment for hurs

Historical gridded reference: Here we use ERA5-RCM as the historical reference. We compared the 12-month climatology of the ERA5-RCM with observations from 5 manned stations in Singapore, and the results (Figure 9.31) show that ERA5-RCM can provide a reasonably realistic gridded reference for hurs.

Bias-adjusted historical climatology: Models tend to underestimate the hurs in Jan-April, and bias-adjusted simulations match with the reference (Figure 9.32).

Bias-adjusted future climatology: Models tend to underestimate the magnitude in the future period during Jan- April. Adjusted simulations tune up the magnitude which becomes more realistic (Figure 9.33). Moreover, the seasonal cycle is adjusted to match better with the observation reference.

Climate change largely preserved by bias adjustments: Models tend to project reduction of the hurs (-2.5% in value as in Figure 9.34, -3% in percentage changes) across all seasons except in May. Bias adjustments largely preserve the change.

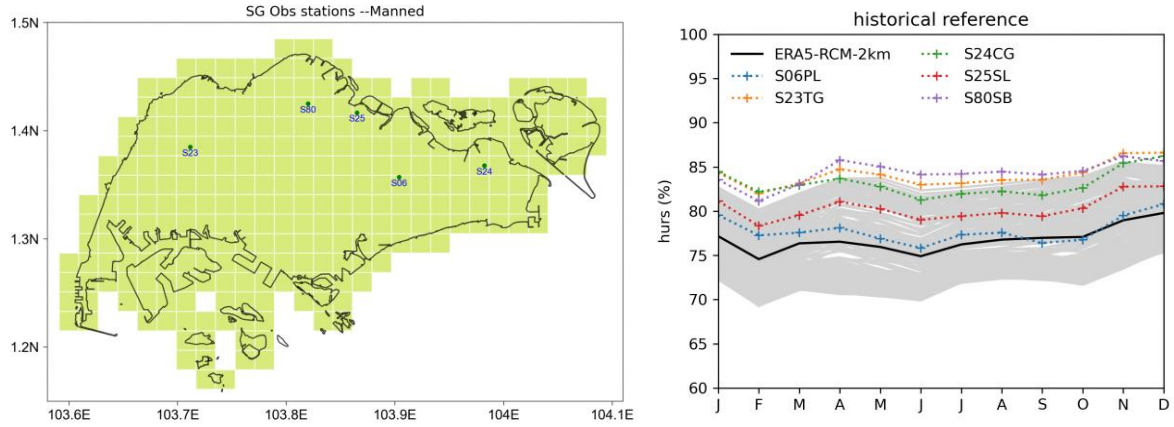

Figure 9.31. a. Map of manned stations in Singapore. b. 12-month climatology of hurs in the historical period (1995-2014) from 5 manned stations (dotted) and from ERA5-RCM gridcells across Singapore (black is the gridcell mean) at a 2km resolution.

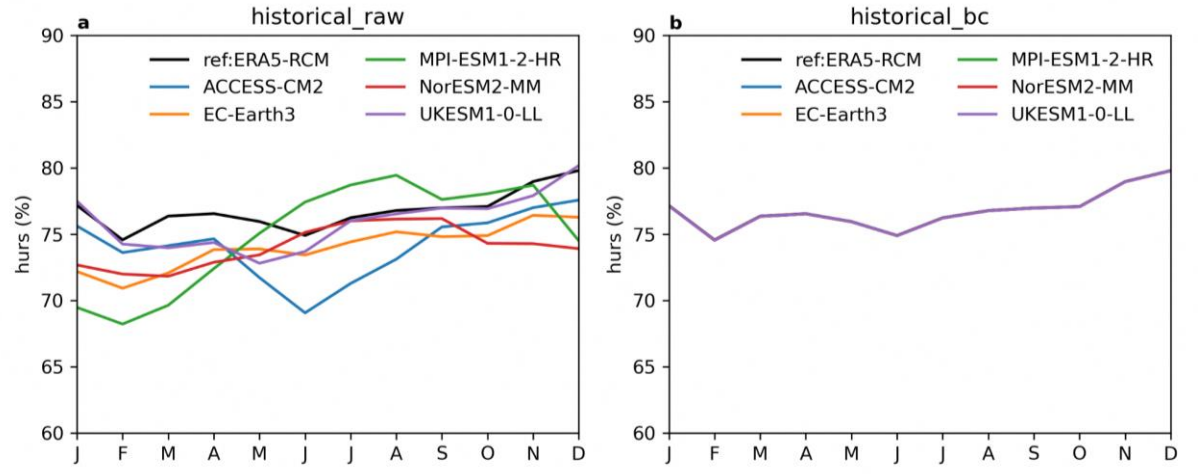

Figure 9.32: Singapore domain-averaged hurs in the historical period (1995-2014) at a 2km resolution. a. observation reference (ERA5-RCM) and raw simulations. b. similar to a, but plotting bias-adjusted simulations.

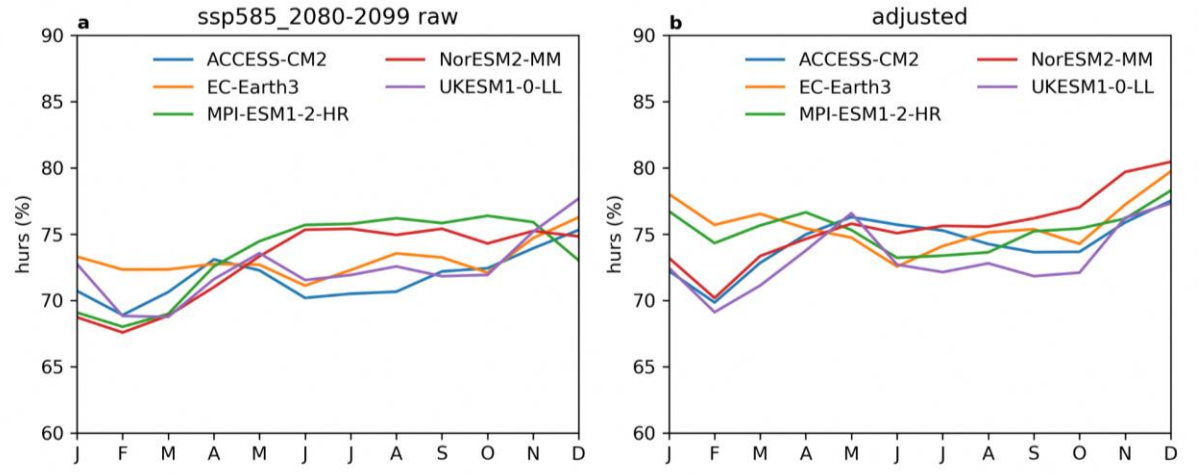

Figure 9.33: Singapore domain-averaged hurs in the future period (2080-2099) under the SSP585 scenario at a 2km resolution. a. raw simulations. b. bias-adjusted simulations.

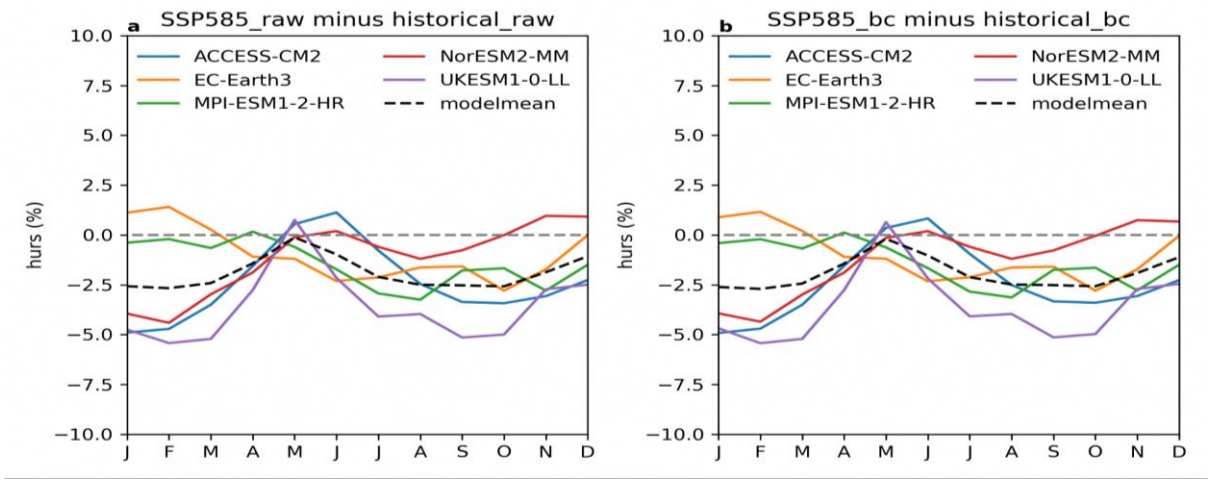

Figure 9.34: Changes in the Singapore domain-averaged hurs from the historical period (1995-2014) to the future period (2080-2099) under the SSP585 scenario at a 2km resolution. a. raw simulations. b. bias-adjusted simulations.

Climate change patterns preserved by bias adjustments: Here future change of hurs projected by UKESM1-0-LL (Figure 9.35) in both raw and adjusted simulations show a larger reduction of hurs in the north-western Singapore compared to the south-eastern Singapore. Note that bias adjustments preserve the spatial feature of the change.

Bias-adjusted distribution: Distributions of modeled hurs are adjusted to the reference distribution (ERA5-RCM) for the historical period (Figure 9.36). Under warming, distributions of overestimated and underestimated July hurs are all adjusted accordingly.

Trend in annual mean hurs: Here we show time series of hurs in models are adjusted up to match observation mean in the historical period (Figure 9.37). Also the variability range of simulations is reduced to match the observation. In the future period, adjusted time series provide more realistic projection with adjusted mean and variability. Bias adjustment also preserve the trend.

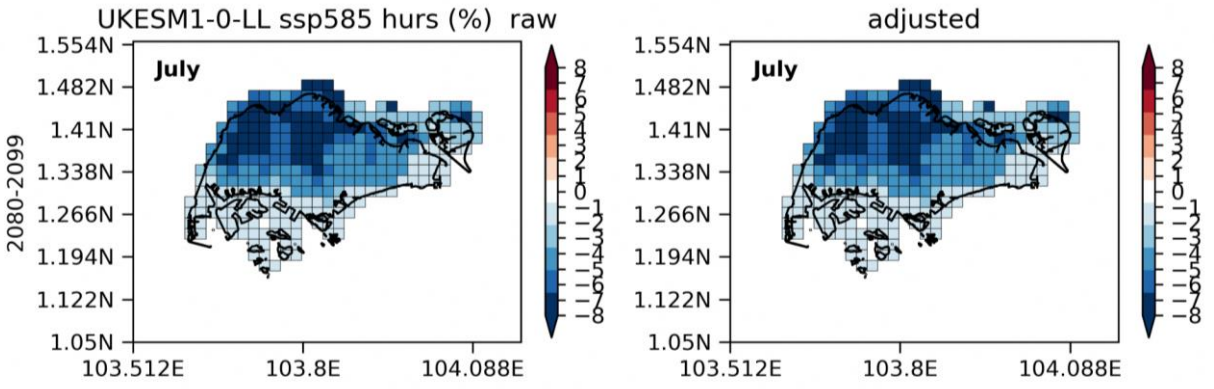

Figure 9.35: UKESM1-0-LL simulated 2km resolution Singapore July hurs change from the historical period (1995-2014) to the future period (2080-2099) under the SSP585 scenario. a. raw simulation. b. bias-adjusted simulations.

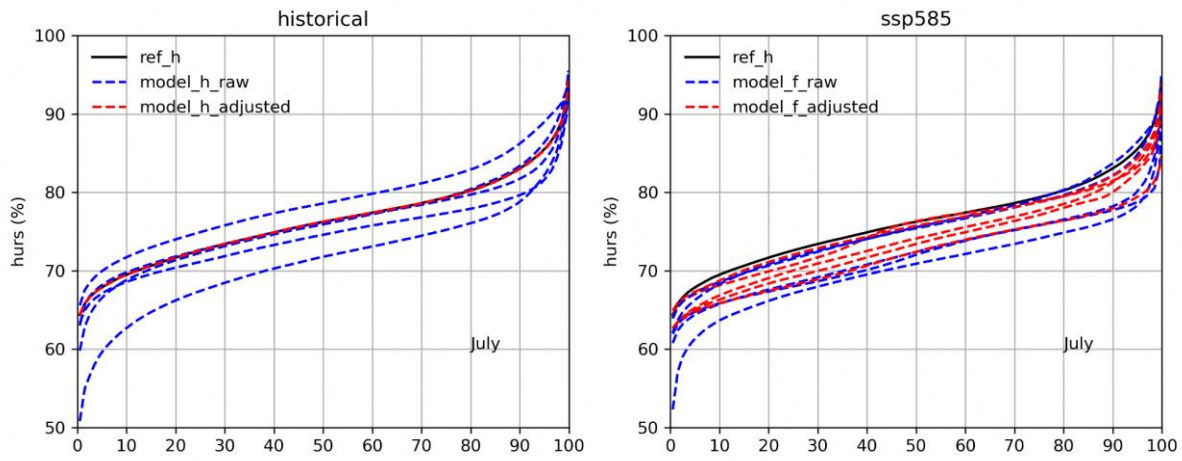

Figure 9.36: a. July CDF of hurs at 2km resolution gridcells across Singapore for the historical period (1995-2014). The reference is the station kriged rainfall. b. July CDF for the future period (2080-2099) under the SSP585 scenario.

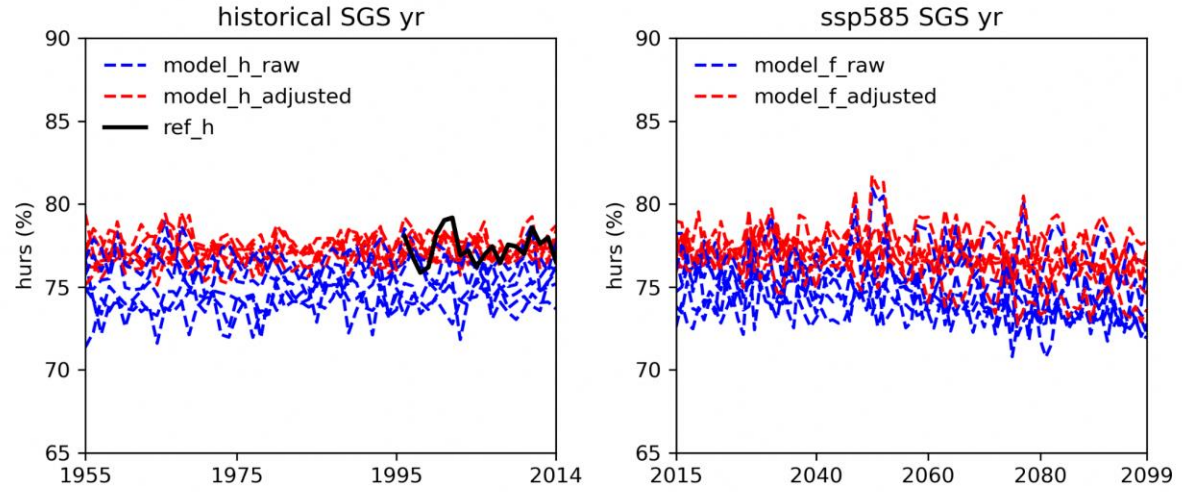

Figure 9.37: a. 8km resolution Singapore domain-averaged hurs in the historical period. b. hurs in the future period under the SSP585 scenario. Observation reference is in black. Raw simulations are in blue, and bias-adjusted simulations are in red.

9.9 Results: bias-adjustment for sfcWind

Historical gridded reference: We use the ERA5-RCM as the observation reference. We compared sfcWind climatology of all gridcells over Singapore from ERA5-RCM with 21 station data. Results (Figure 9.38) show that station sfcWind are largely within/overlap with the ERA5-RCM range, which suggests that ERA5-RCM data is a suitable product to provide a gridded estimate for sfcWind.

Bias-adjusted historical climatology: Surface wind speed over Singapore shows stronger wind during the monsoon seasons (Northeast and Southwest Monsoon season) and weaker wind during the intermonsoon transition period (Figure 9.39). Models overall overestimate the magnitude of sfcWind during the winter monsoon season. Bias-adjusted simulations match with the observation reference.

Bias-adjusted future climatology: Models overestimate the sfcWind in the winter monsoon season. Here adjusted future projection of sfcWind is tuned down for winter season (Figure 9.40).

Climate change preserved by bias adjustments: As to the future change, models project increase in the sfcWind (~0.5m/s in Figure 9. 41, or ~12% change) during the monsoon seasons (DJFM, and JJAS) except in the intermonsoon seasons (May, and Nov).

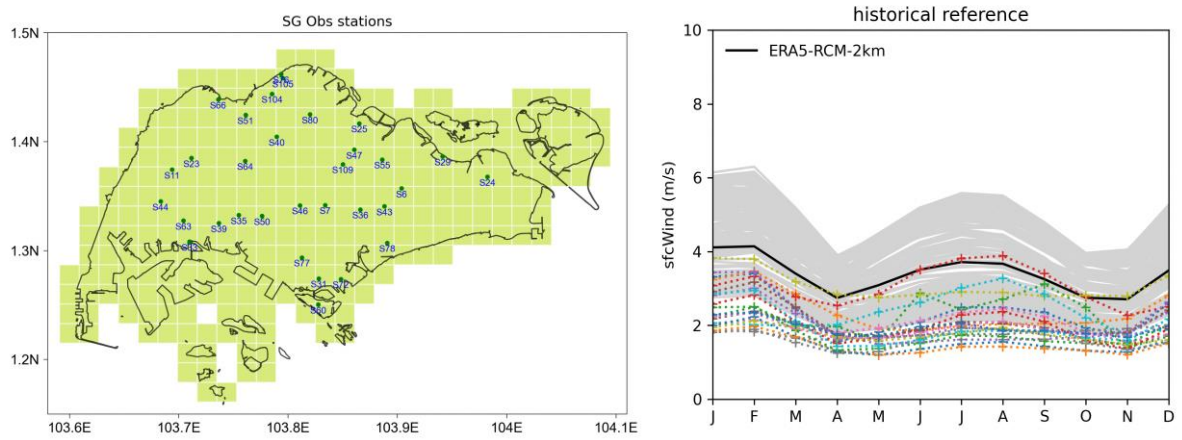

Figure.9.38 a. map of 21 stations on sfcWind. b. 12-month climatology in the historical period of station sfcWind (dotted) versus gridcells from ERA5-RCM (black is the gridcell mean) over Singapore.

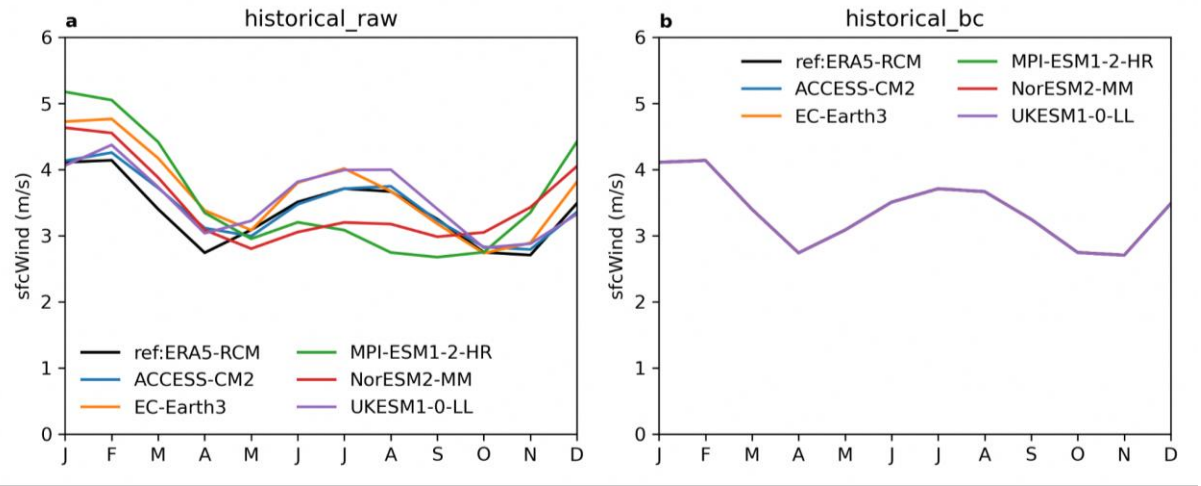

Figure 9.39: 12-month climatology of Singapore domain-averaged sfcWind in the historical period (1995-2014) at a 2km resolution. a. observation reference (ERA5-RCM, black) and raw simulations. b. similar to a, but plotting bias-adjusted simulations.

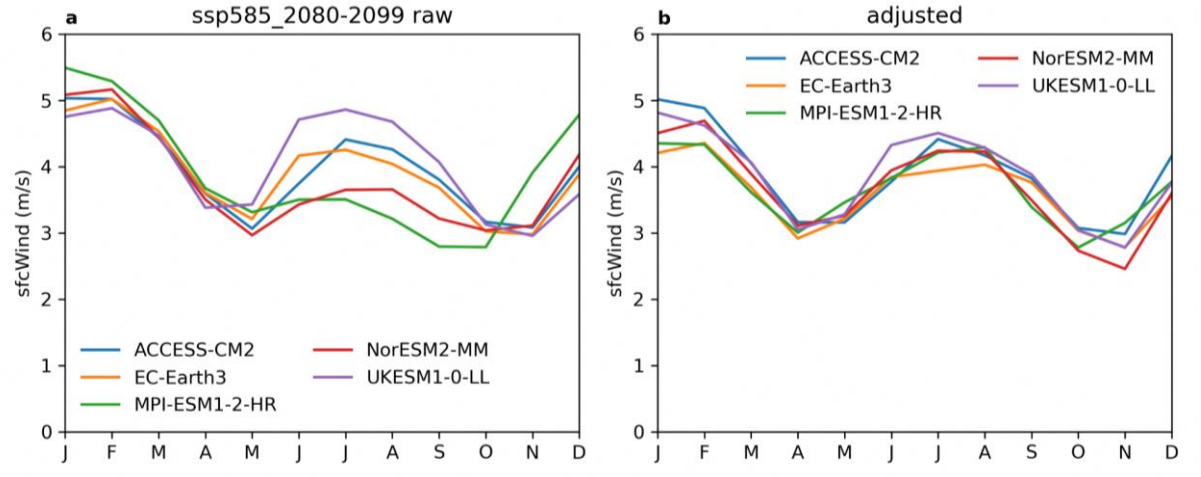

Figure 9.40: Singapore domain-averaged sfcWind in the future period (2080-2099) under the SSP585. a. raw simulations. b. bias-adjusted simulations.

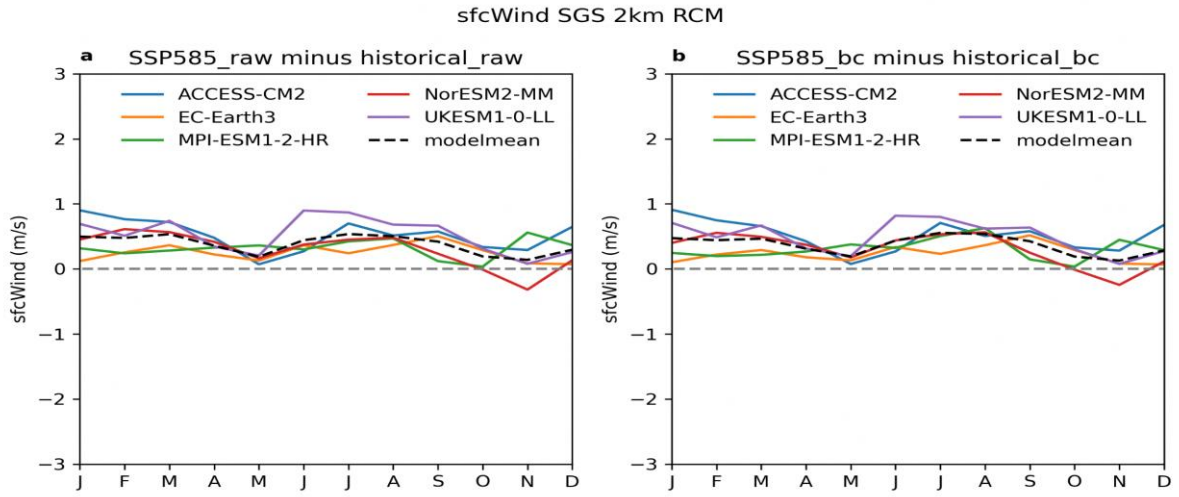

Figure 9.41: Percentage changes in the Singapore domain-averaged sfcWind from the historical period (1995-2014) to the future period (2080-2099) under the SSP585 scenario. a. raw simulations. b. bias-adjusted simulations.

Climate change patterns preserved by bias adjustments: Future change of sfcWind shows a larger increase at the coastal area of Singapore (Figure 9.42). Bias adjustment largely preserves the future change.

Bias-adjusted distribution: Distributions of modeled sfcWind are adjusted to the reference distribution (ERA5-RCM) for the historical period (Figure 9.43). Under warming, distributions of overestimated and underestimated July sfcWind are all adjusted accordingly.

Trend in annual mean sfcWind: Here we show the annual mean sfcWind in models are reduced to match observation mean in the historical period (Figure 9.44). Also the variability range of the adjusted simulations is similar to the observation. In the future period, adjusted time series provide more realistic projection with adjusted mean and variability. Bias adjustment also preserves the trend.

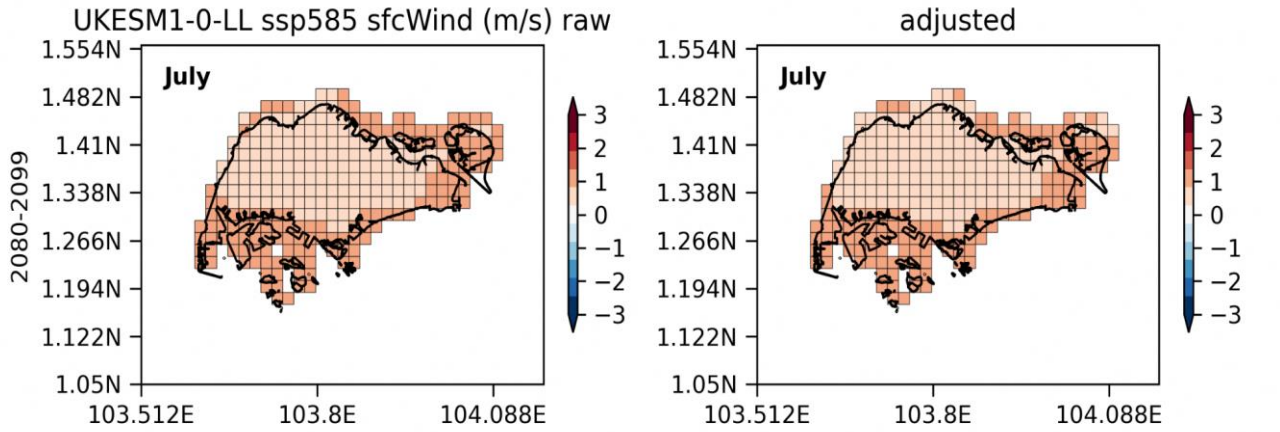

Figure 9.42: UKESM1-0-LL simulated 2km resolution Singapore July sfcWind change from the historical period to the future period under the SSP585 scenario. a. raw simulation. b. bias-adjusted simulations.

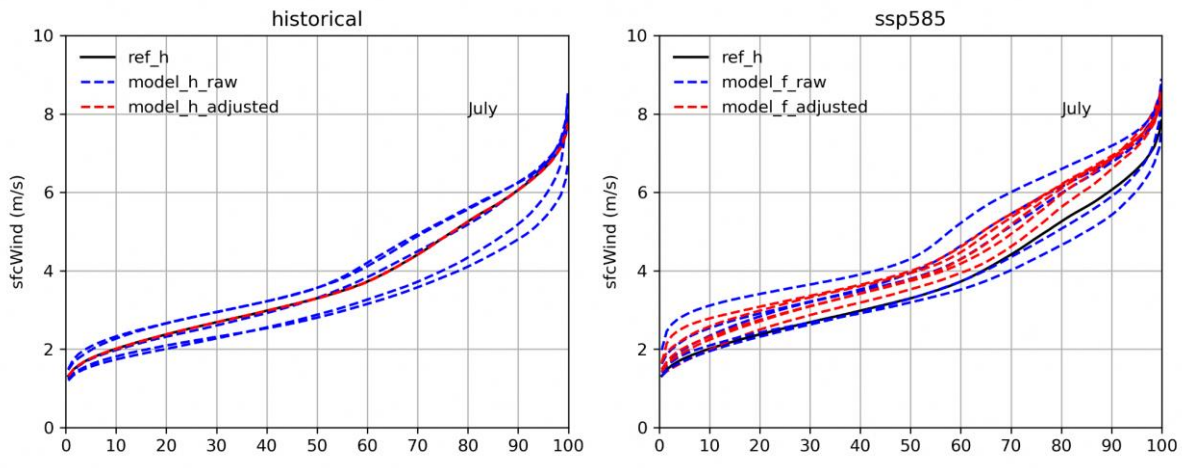

Figure 9.43: a. July CDF of sfcWind at 2km resolution gridcells across Singapore for the historical period (1995-2014). The reference is ERA5-RCM. b. July CDF for the future period (2080-2099) under the SSP585 scenario.

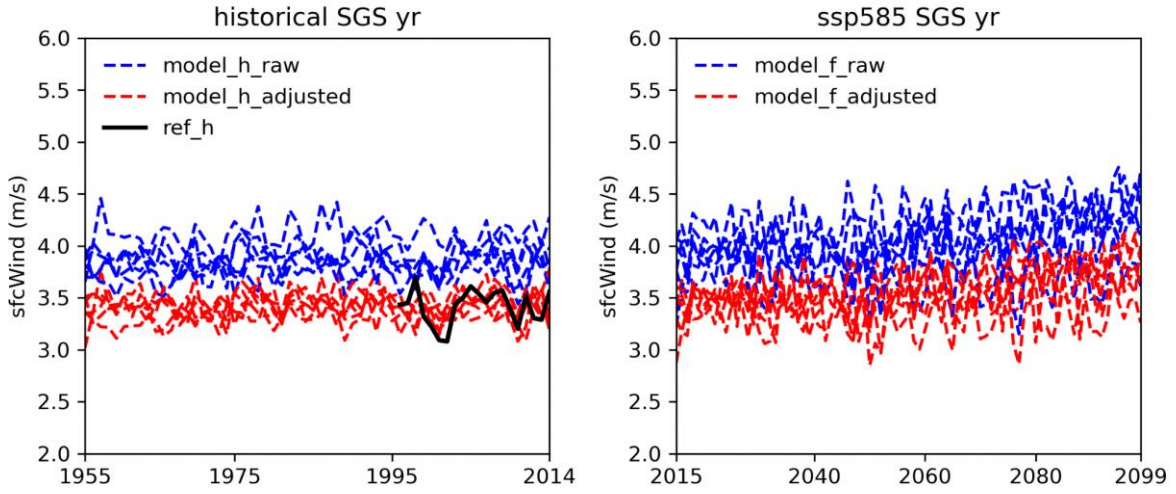

Figure 9.44: a. 8km resolution Singapore domain-averaged sfcWind in the historical period. sfcWind in the future period under the SSP585 scenario. Observation reference is in black. Raw simulations are in blue, and bias-adjusted simulations are in red.

9.10 Results: bias-adjusted climate impact indices

9.10.1 Derived extreme indices

Table 9.8 showcases the extreme indices calculated for impact studies based on essential variables, such as daily precipitation, maximum temperature, and minimum temperature.

The application of bias adjustments to those base variables leads to a substantial reduction in biases within the derived indices. This demonstrates that the bias adjustments not only enhance the accuracy and reliability of the raw model output but also ensure that the resulting indices accurately represent the desired characteristics of extreme events.

By mitigating biases in the derived indices, we can now have greater confidence in the validity and usefulness of the data for understanding and addressing extreme climate events. This improvement in data quality is of great importance in various fields, from climate research to policy-making and disaster preparedness.

Here we will show two examples of the derived frequency indices. One is the CWD (consecutive wet days), the other one is the R20mm (Number of very heavy precipitation days when pr>=20mm).

Table 9.8: Derived indices after the bias correction

Variables	Unit	Base variable	Description
RX1day	mm	pr	Maximum 1-day precipitation
RX5day	mm	pr	Maximum 5-day precipitation
PRCPTOT	mm	pr	Total precipitation during Wet Days
R10mm	days	pr	Number of heavy precipitation days (pr>=10mm)
R20mm	days	pr	Number of very heavy precipitation days (pr>=20mm)
CWD	days	pr	Maximum consecutive wet days (pr>=1mm)
CDD	days	pr	Maximum consecutive dry days (pr<1mm)
TXx	°C	tasmax	Maximum daily maximum temperature
TXn	°C	tasmax	Minimum daily maximum temperature
TNx	°C	tasmin	Maximum daily minimum temperature
TNn	°C	tasmin	Minimum daily minimum temperature

9.10.2 CWD and its future change

Let's consider the example of the consecutive wet days (CWD) index. It measures the maximum number of consecutive days with precipitation greater than or equal to 1mm, is an important measure of rainfall frequency. In Singapore, the CWD exhibits a seasonal cycle, with longer durations of wet days observed in April and during the winter monsoon season, and shorter durations during the dry (summer monsoon) season. This seasonal pattern generally aligns with the monthly mean rainfall climatology.

During the historical period, the SINGV-RCMs tend to underestimate the duration of wet days compared to the observation reference, with an average difference of around 3 days (observation reference: ~7 days). It is important to note that direct bias correction for the CWD index was not performed in this study, hence a perfect match is not expected. However, the bias-adjusted model simulations exhibit a much closer agreement with the observations (Figure 9.45), indicating that the bias adjustments have significantly improved the accuracy of the model outputs for the CWD index.

The close agreement between the bias-adjusted model simulations and the observation reference for the CWD index suggests that the bias correction approach employed in this study has effectively addressed the systematic biases in the SINGV-RCMs, leading to more reliable and realistic estimates of the duration of wet days.

As to the future change, raw model simulations also underestimate the CWD (Figure 9.46). And bias-adjusted simulations tuned up to show a more realistic magnitude of CWD for the future period.

The raw CWD shows a reduction (i.e., a shorter duration of wet days) under warming (Figure 9.47). After bias adjustments, the CWD values are tuned up, and the reduction range is also enlarged.

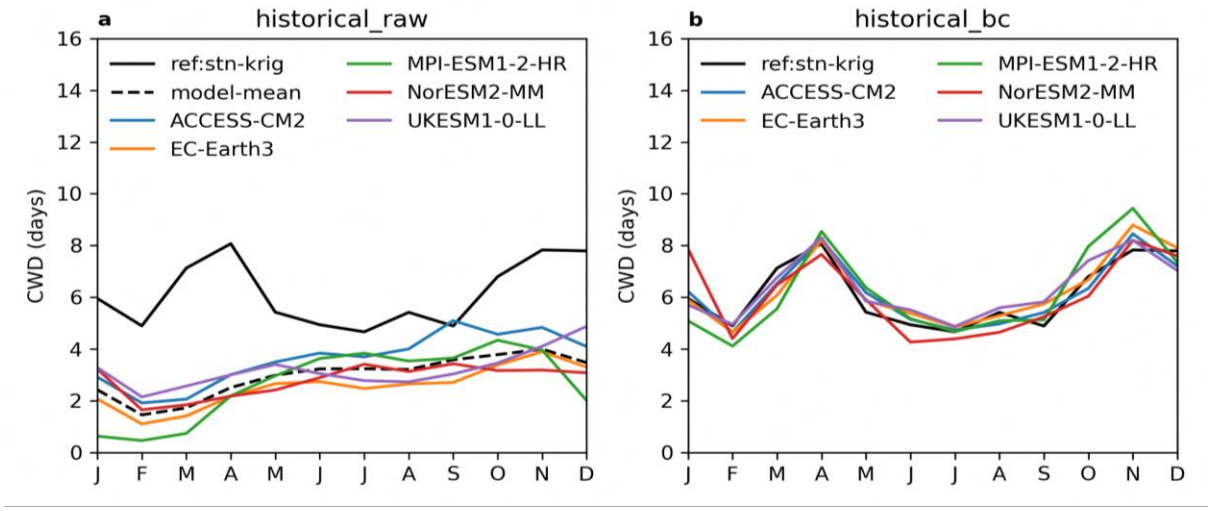

Figure 9.45: Singapore domain-averaged CWD in the historical period (1995-2014). a. observation reference (station krig pr) and raw simulations. b. similar to a, but plotting bias-adjusted simulations. Note that the value of CWD represents the wet days starting from individual month instead of truncated to the given month.

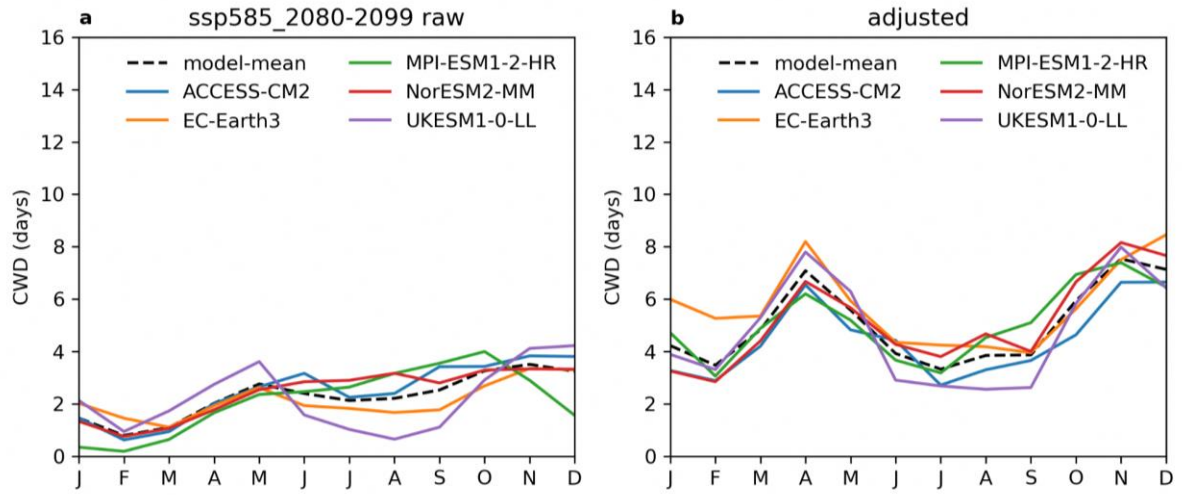

Figure 9.46: Singapore domain-averaged CWD in the SSP585 future period (2080-2099). a. raw simulations. b. bias-adjusted simulations.

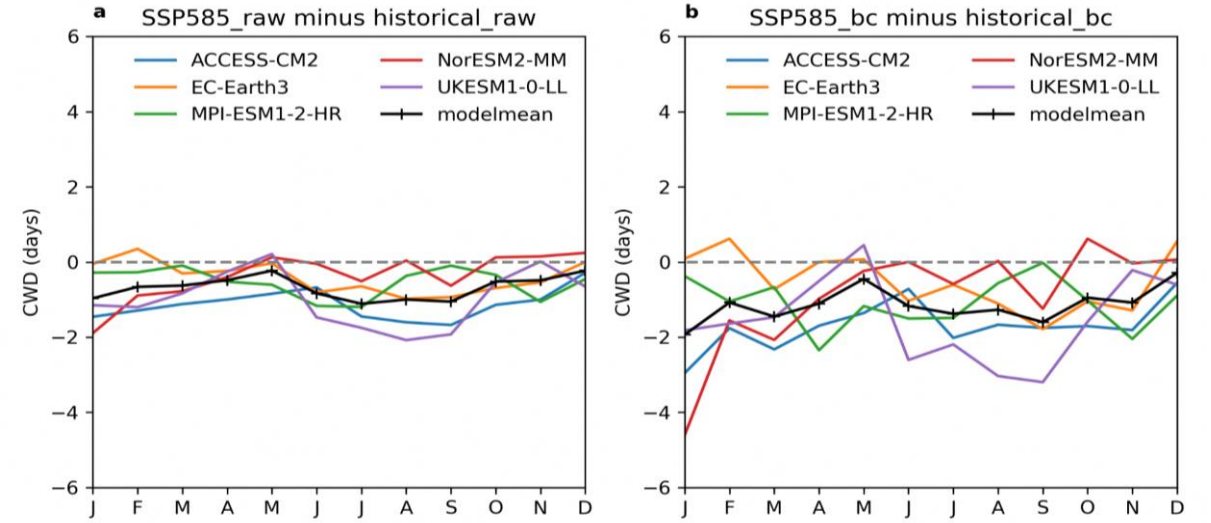

Figure 9.47: Changes in the Singapore domain-averaged CWD from the historical period (1995-2014) to the future period (2080-2099) under the SSP585 scenario. a. raw simulations. b. bias-adjusted simulations.

9.10.3 R20mm and its future changes

Here we show the other example of the frequency-based extreme index R20mm (Number of very heavy precipitation days (pr>=20mm), in days in unit). The dry season (JJAS) shows fewer days of the R20mm, while the wet season (NDJ and April) shows more days of R20mm. It overall follows the seasonal cycle of the mean rainfall.

Figure 9.48 shows that models tend to underestimate the R20mm in JFMA, but overestimate the R20mm in JJAS. The bias-adjusted simulations match R20mm with the observation very well. Note that the R20mm was not directly bias-adjusted but derived from the bias-adjusted pr. It indicates the bias adjustment in base variables like pr are successful and useful for impact studies.

Figure 9.49 showed the future R20mm under the SSP585 scenario. Future simulations tend to have similar biases as the historical period. After bias adjustments, JFMA season R20mm are tuned down, and the JJAS season R20mm are tuned down.

Figure 9.50 showed the future change of R20mm. The reduction in heavy rainfall days are mainly in the JJAS season. After the bias adjustment, the R20mm in the JJAS season are tuned down and the changes are also reduced.

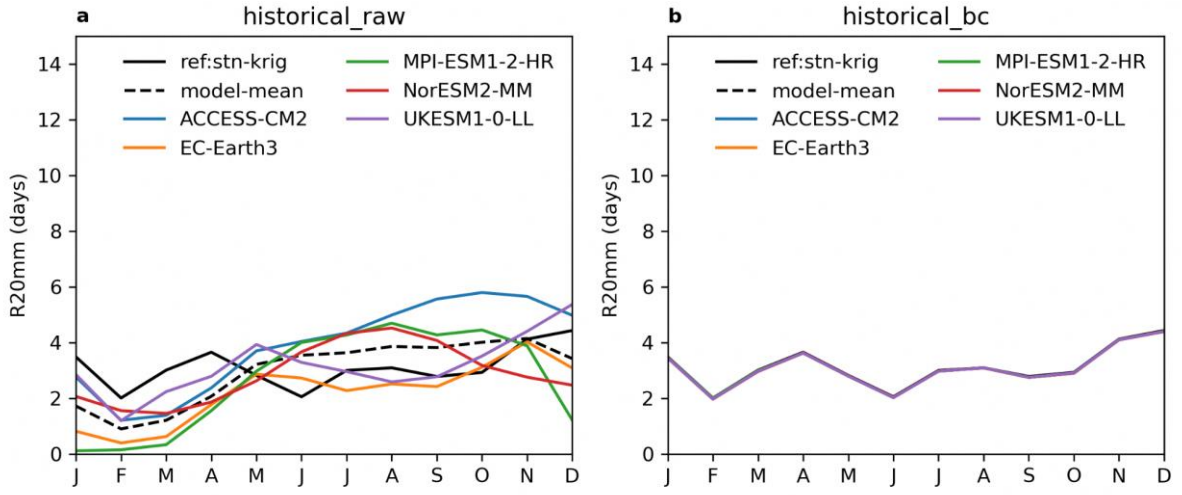

Figure 9.48: Singapore domain-averaged R20mm in the historical period (1995-2014) at a 2km resolution. a. observation reference (station krig pr) and raw simulations. b. similar to a, but plotting bias-adjusted simulations.

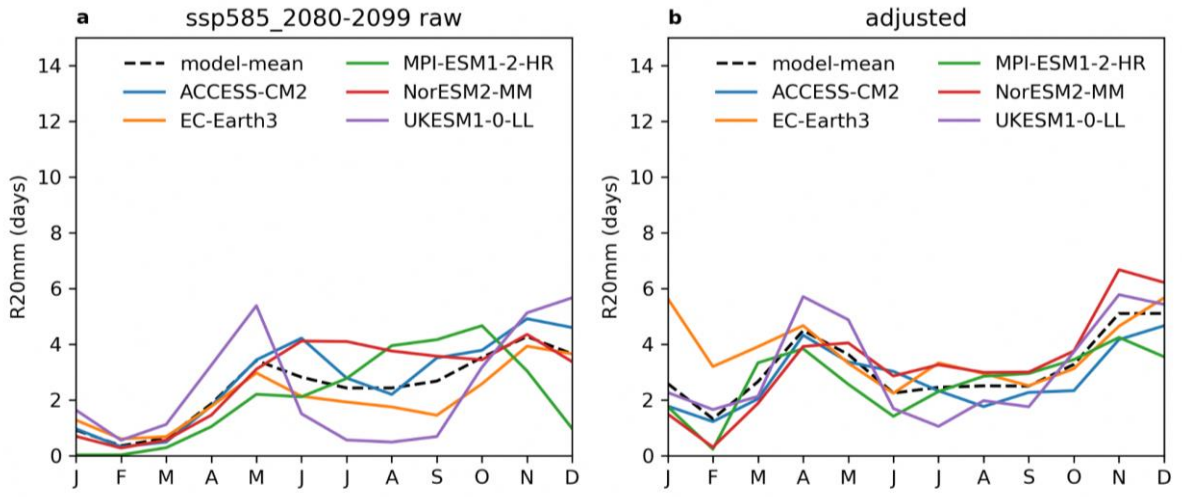

Figure 9.49: Singapore domain-averaged R20mm in the future period (2080-2099) under the SSP585 scenario. a. raw simulations. b. bias-adjusted simulations.

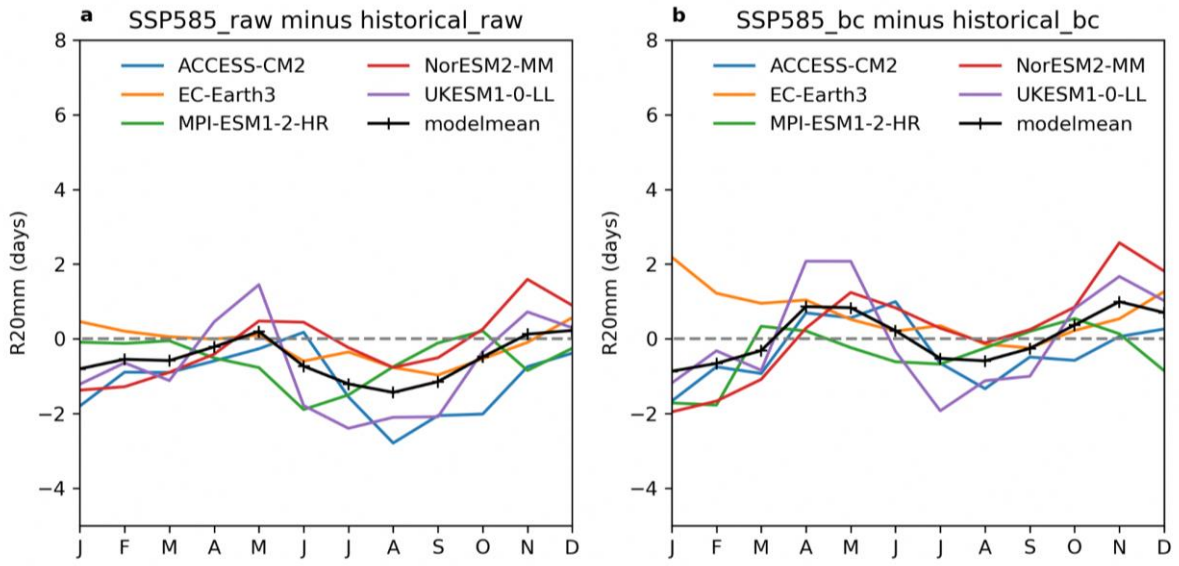

Figure 9.50: Percentage changes in the Singapore domain-averaged R20mm from the historical period (1995-2014) to the future period (2080-2099) under the SSP585 scenario at a 8km resolution. a. raw simulations. b. bias-adjusted simulations.

9.11 Evaluations using pseudo reality experiments

We showed in above results that bias adjustments are very useful to remove the systematic biases in models, provide more realistic simulations, and largely preserve the change and long-term trend. We have to acknowledge that bias-adjusted projections still have inevitable uncertainties given that we do not know what the actual future will look like in the reality. To provide more confidence, here we conduct an evaluation using a pseudo reality experiment. The main objective of this experiment was to assess the performance of the bias adjustment method by comparing the bias-adjusted simulations with a designated reference model that represents an alternative plausible reality.

The experiment involved selecting one CMIP6 model, specifically MPI-ESM1-2-HR, as the reference model, while the other four CMIP6 models were treated as test models (Table 9.9). The study domain focused on the West Maritime Continent (WMC) with a spatial extent of [7S-10N, 93-110W]. For the GCMs with a resolution of 1.5 degrees, this corresponds to a grid size of 12x12 cells. The historical period from 1995 to 2014 was chosen as the base period, while the future change period spanned from 2080 to 2099, considering the SSP585 scenario for analyzing the warming future.

The evaluation process involved comparing the differences between the reference model and the test models in both the historical period and future scenarios. The bias correction method was applied to the test models using the historical data from the reference model. The results demonstrated that the bias-adjusted simulations effectively reduced the biases present in the historical period, bringing them closer to the reference model. Furthermore, the adjusted future projections showed improved agreement with the actual future projections of the reference model.

The successful performance of the bias correction method in this evaluation, using the ISIMIP3 bias correction approach, provided increased confidence in the bias-adjusted downscaling outputs. This evaluation process contributes to reducing uncertainties associated with the bias adjustment procedure and enhances the reliability of the projections for the impact assessment and decision-making processes.

Table 9.9: CMIP6 model information for the bias adjustment tests

Category	CMIP6 model	ensemble ID	historical period	SSP585 period
reference model	MPI-ESM1-2-HR	r1i1p1f1	1850-2014	2015-2100
test model	ACCESS-CM2	r1i1p1f1	1850-2014	2015-2100
test model	EC-Earth3	r1i1p1f1	1850-2014	2015-2100
test model	MIROC6	r1i1p1f1	1850-2014	2015-2100
test model	NorESM2-MM	r1i1p1f1	1850-2014	2015-2100

9.11.1 Evaluation for the mean climatology

The WMC domain-averaged climatology for surface wind speed (sfcWind) from individual models was adjusted to match the reference model during the historical period, as shown in Figure 9.51d. The bias adjustment process aimed to correct the discrepancies between the individual models and the reference model. By applying the bias adjustment, the future projections of sfcWind from the test models became more aligned with the future projections of the reference model, as depicted in Figure 9.51d.

It is important to note that the specific adjustments for each model depended on the biases observed in the historical period. In the case of MIROC6, this model exhibited an underestimation of sfcWind compared to the reference model during the historical period. Consequently, the bias-adjusted future sfcWind in MIROC6 was shifted upwards from the raw climatology (green), bringing it closer to the actual future projections of the reference model (black). Furthermore, the bias-adjusted simulations demonstrated a significant preservation of the future changes of individual models, as illustrated in Figure 9.51f. This indicates that the bias adjustment process successfully retained the essential characteristics of the future changes projected by the models while reducing systematic biases.

Overall, the bias adjustment procedure effectively improved the realism and accuracy of the sfcWind projections from the test models, aligning them more closely with the reference model.

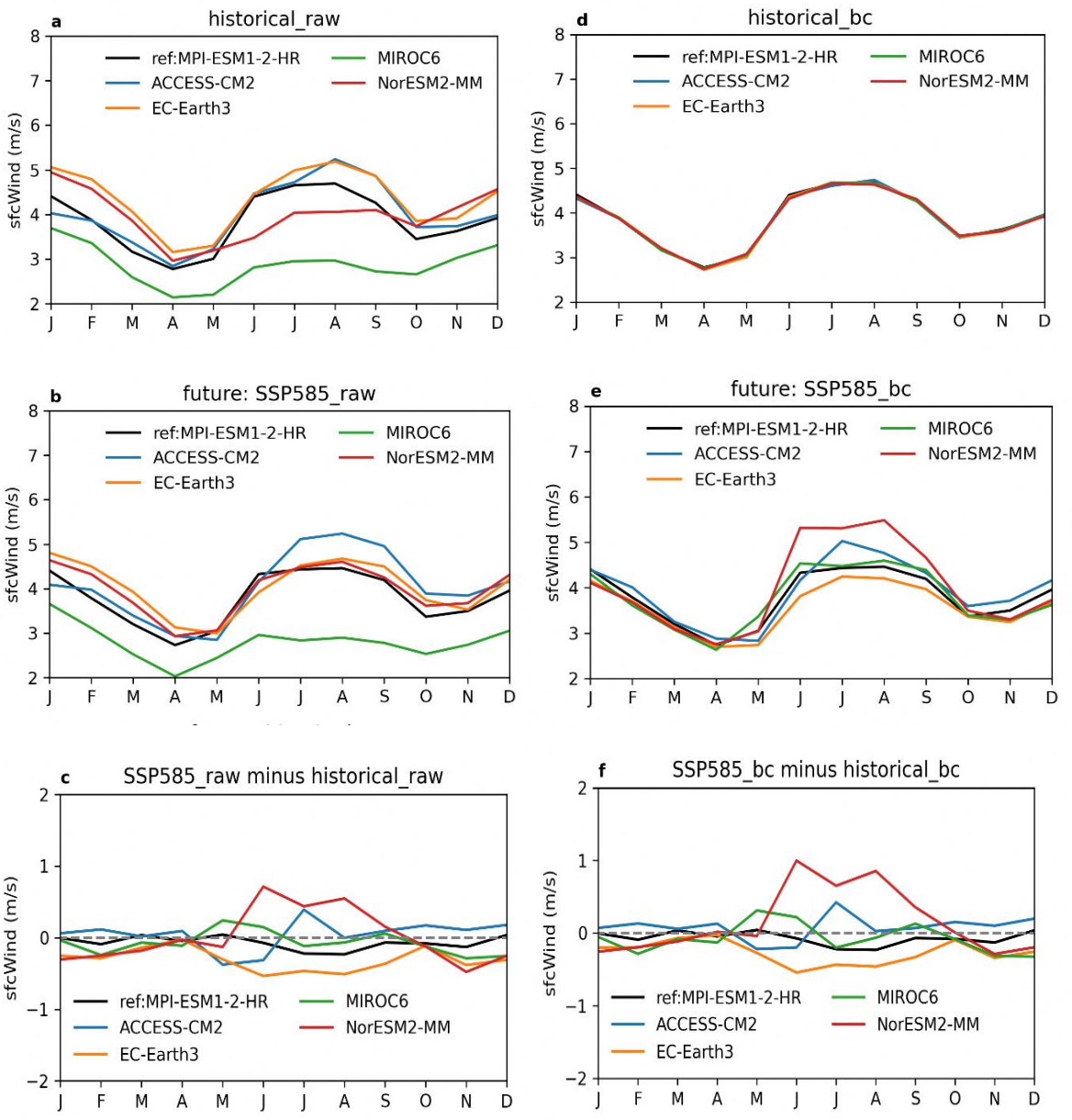

Figure 9.51: WMC domain averaged sfcWind in the historical period (a,d). Raw model outputs are in a. Bias corrected model outputs are in d. WMC domain averaged sfcWind in the future period (b,d). Raw model outputs are in b. Bias corrected model outputs are in d. WMC domain averaged sfcWind changes (2080-2099 minus 1995-2014) (c,f). Raw model outputs are in c. Bias corrected model outputs are in f.

9.11.2 Evaluation for the spatial pattern

The spatial pattern analysis of surface wind speed (sfcWind) in the WMC domain revealed certain characteristics for the month of July. Specifically, the central land area of the WMC tended to have lower wind speeds, while higher wind speeds were observed over the open ocean area, as depicted in Figure 9.52. This spatial distribution of wind speed is indicative of the prevailing atmospheric circulation patterns during that month.

Considering the future projections under warming from the reference model, a distinct change in the spatial pattern of sfcWind was observed. The reference model projected reduced sfcWind in the northern part of the WMC, indicating a weakening of wind speeds in that region. Conversely, enhanced sfcWind was projected near the equator, suggesting an increase in wind speeds in that area due to the influence of climate change, as illustrated in Figure 9.52.

This spatial pattern analysis provides insights into the potential changes in wind patterns and intensities within the WMC region under future warming scenarios. It demonstrates that the reference model's projections capture the expected shifts in wind speed distribution, allowing for a better understanding of the potential impacts of climate change on wind patterns in the WMC domain.

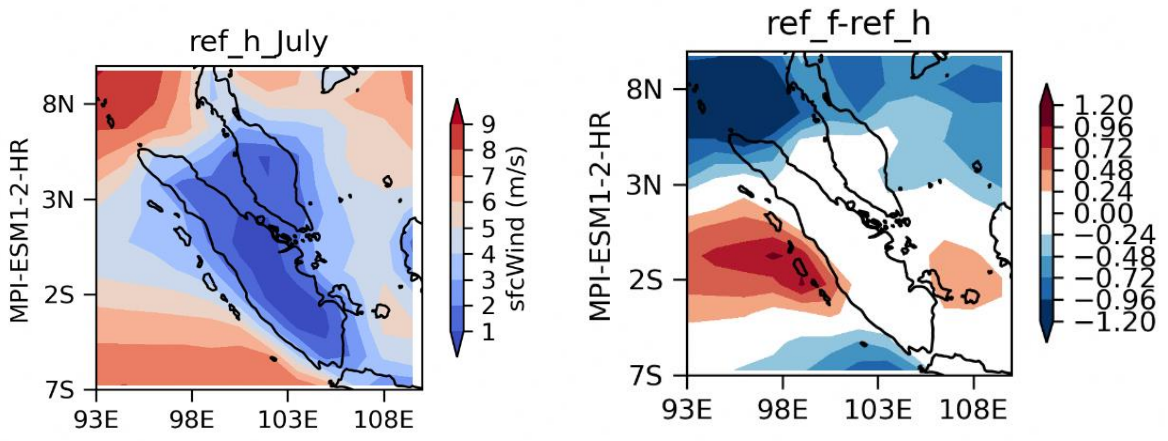

Figure 9.52: a. WMC domain sfcWind (July) in the historical period of the reference model (MPI-ESM1-2-HR). b. Future changes in WMC domain sfcWind projected by the reference model.

During the historical period, the four test models (including ACCESS-CM2) generally exhibit a similar spatial pattern of surface wind speed (sfcWind) compared to the reference model, with some variations in magnitude. In the case of ACCESS-CM2, it tends to overestimate sfcWind in the central WMC region, as illustrated in Figure 9.53.

To address the overestimation issue and improve the agreement with the reference model, bias adjustment was applied to the sfcWind simulations from ACCESS-CM2. The bias-adjusted sfcWind values demonstrate a better match with the reference model, indicating that the adjustment successfully mitigated the overestimation bias in the central WMC region. The comparison between raw and bias-adjusted sfcWind highlights the effectiveness of the bias adjustment method in reducing discrepancies and improving the agreement with the reference model. By correcting the systematic biases in the sfcWind simulations, the bias-adjusted results provide a more reliable representation of the historical wind patterns in the WMC domain.

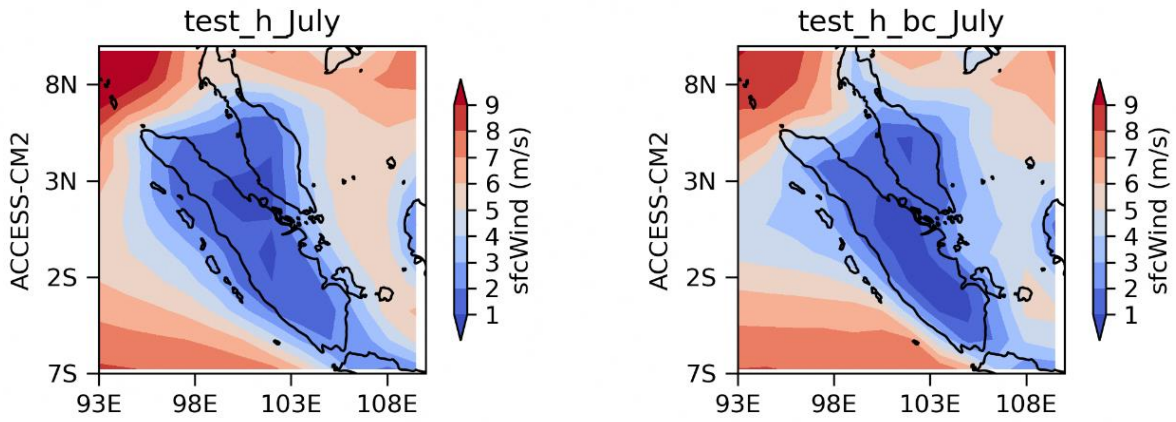

Figure 9.53: a. WMC domain sfcWind (July) in the historical period of raw test model (ACCESS-CM2). b. bias-adjusted test model.

In terms of the future changes in July surface wind speed (sfcWind) over the WMC, the four test models (including ACCESS-CM2) exhibit varying patterns. For instance, ACCESS-CM2 projects an enhanced sfcWind over the southeastern WMC region and a reduced sfcWind over the northwestern WMC region, as depicted in Figure 9.54.

After applying the bias adjustment to the sfcWind simulations from the test models, the spatial changes in sfcWind are largely preserved in the bias-adjusted results. This means that the bias adjustment process did not significantly alter the projected spatial pattern of sfcWind changes. The bias-adjusted simulations still reflect the enhanced sfcWind over the southeastern WMC and reduced sfcWind over the northwestern WMC, in line with the original model projections.

This preservation of the spatial changes in sfcWind after bias adjustment provides additional confidence in the reliability of the bias-adjusted simulations for assessing future wind patterns over the WMC. It suggests that the bias adjustment method successfully corrected the systematic biases in the models without introducing substantial distortions to the projected changes.

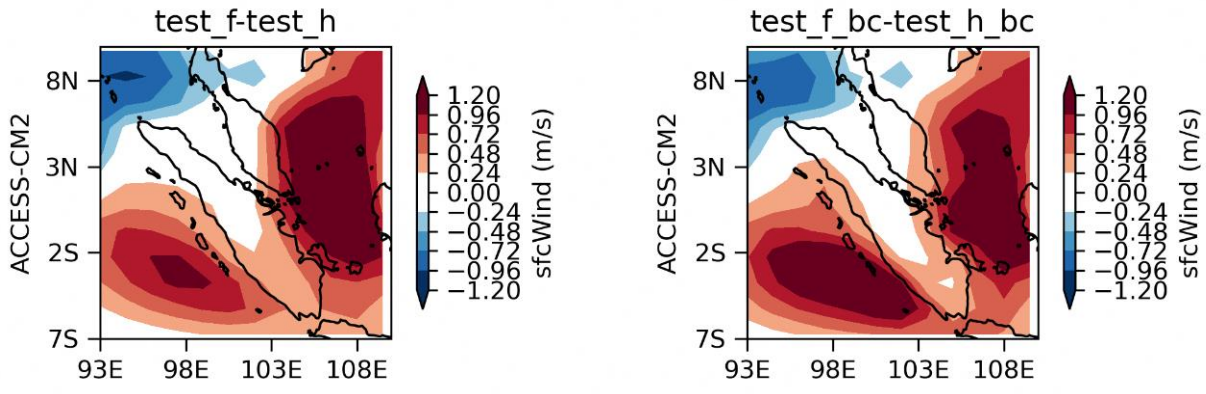

Figure 9.54: a. future changes in WMC domain sfcWind projected by raw the test model (ACCESS-CM2). b. bias-adjusted test model.

9.12 Summary

Our high-resolution regional climate model (RCM) simulations, conducted at resolutions of 8km and 2km, have demonstrated excellent performance over the Maritime Continent. However, these high-resolution RCMs exhibit slight model biases when compared to local observations specifically within Singapore. To ensure that we provide appropriate simulation data for local climate change impact studies, we have conducted bias adjustments for several key climate variables. These variables include tas (near-surface air temperature), tasmax (maximum air temperature), tasmin (minimum air temperature), pr (precipitation), hurs (relative humidity), and sfcWind (surface wind speed). By applying bias adjustments to these selected variables, we aim to align the RCM simulations more closely with the observed local climate conditions in Singapore.

In order to perform bias corrections, it is crucial to have gridded observation reference data that is specifically tailored to the high-resolution (8km and 2km) scale required for Singapore. However, finding existing observation products at such fine resolutions can be challenging. To overcome this limitation, we adopted a two-step approach. For rainfall (pr), we utilized data from 28 long-term rainfall stations to create gridded precipitation data at resolutions of 2km and 8km using advanced kriging techniques. This allowed us to generate gridded precipitation reference datasets that closely represent the spatial variability of rainfall in Singapore. Evaluations conducted on the kriged precipitation data demonstrated its suitability as a reference dataset, as it exhibited strong consistency with the station precipitation data. For other variables, such as temperature (tas, tasmax, tasmin), relative humidity (hurs), and surface wind speed (sfcWind), the number of available

long-term stations was insufficient for directly converting them into gridded products. Therefore, we used the 25km-resolution ERA5 reanalysis dataset to drive the 8km and 2km resolution RCMs. The output within the Singapore domain from the ERA5-RCM simulations served as the gridded reanalysis reference. Evaluations conducted on the ERA5-RCM data revealed its suitability as a reference dataset, as it demonstrated excellent consistency with the available station data across Singapore. These gridded reference datasets, derived from kriging of station data for precipitation and the ERA5-RCM simulations for other variables, currently represent the best options available for conducting bias corrections in our study. If new observation products become available at higher resolutions in the future, we can update the historical reference accordingly in subsequent studies.

For the bias adjustment process in the V3 study, we recognized the need for advanced features beyond the straightforward quantile-mapping based bias adjustment methods used in V2. These new requirements included preserving trends, correcting rainfall frequency, and customizing distribution fits for each variable, among others. To meet these demands, we implemented the latest and widely used ISIMIP3 bias adjustment methods. The results of the bias adjustment process demonstrated the successful removal of biases in the adjusted historical simulations. Additionally, the future simulations showed improved realism after the adjustments. Importantly, the adjustments were able to preserve the future change signals present in the raw simulations, ensuring that the projected climate changes remained intact. To provide further confidence in the reliability of the bias adjustments, we conducted pseudo reality experiments. In these experiments, we designated one model as the reference, with known historical and future data. We then applied bias adjustments to the other test models and assessed the performance and added value of the adjustments. The results of these tests revealed that the simulations after bias adjustments were more realistic compared to the raw simulations. By incorporating the advanced features and conducting rigorous evaluations, the bias adjustments performed in the V3 study produced more reliable and accurate climate simulations. These adjusted simulations provide greater confidence in their use for assessing climate change impacts in Singapore.

In addition to the main climate variables, we derived key extreme indices based on certain variables to assess the characteristics of extreme events. For example, we calculated the maximum consecutive wet days (CWD) using the precipitation (pr) data and the number of very heavy precipitation days (R20mm). Our findings indicate that these frequency-based indices (CWD and R20mm) calculated using the raw simulations exhibited biases. However, after applying the bias adjustments, the biases in the CWD and R20mm based on the adjusted simulations were largely removed. This demonstrates the effectiveness of the bias adjustments in improving the accuracy of extreme indices.

In conclusion, the bias adjustments conducted in our study have demonstrated very good performance. We consider bias adjustment to be a crucial step in the post-processing of regional downscaling simulations, as it significantly improves the realism and accuracy of the regional climate model (RCM) outputs. The successful implementation of bias adjustments enhances our confidence in the climate projections and their suitability for assessing and addressing the impacts of climate change in Singapore.

References

Cannon, A.J., Sobie, S.R. and Murdock, T.Q. (2015) Bias correction of GCM precipitation by Quantile mapping: how well do methods preserve changes in quantiles and extremes? J. Climate, 28, 6938–6959. https://doi.org/10.1175/JCLI-D-14-00754.1.

Cannon, A. J, 2017.: Multivariate quantile mapping bias correction: an N-dimensional probability density function transform for climate model simulations of multiple variables, Climate Dynamics, pp. 1–19, https://doi.org/10.1007/s00382-017-3580-6

Frieler, K., Lange, S., Piontek, F., Reyer, C. P. O., Schewe, J., Warszawski, L., Zhao, F., Chini, L., Denvil, S., Emanuel, K., Geiger, T., Halladay, K., Hurtt, G., Mengel, M., Murakami, D., Ostberg, S., Popp, A., Riva, R., Stevanovic, M., Suzuki, T., Volkholz, J., Burke, E., Ciais, P., Ebi, K., Eddy, T. D., Elliott, J., Galbraith, E., Gosling, S. N., Hattermann, F., Hickler, T., Hinkel, J., Hof, C., Huber, V., Jägermeyr, J., Krysanova, V., Marcé, R., Müller Schmied, H., Mouratiadou, I., Pierson, D., Tittensor, D. P., Vautard, R., van Vliet, M., Biber, M. F., Betts, R. A., Bodirsky, B. L., Deryng, D., Frolking, S., Jones, C. D., Lotze, H. K., Lotze- Campen, H., Sahajpal, R., Thonicke, K., Tian, H., and Yamagata, Y., 2017: Assessing the impacts of 1.5 ◦C global warming simulation protocol of the Inter-Sectoral Impact Model Intercomparison Project (ISIMIP2b), Geosci. Model Dev., 10, 4321–4345, https://doi.org/10.5194/gmd-10-4321-2017

Gleick, P. H. (1986). Methods for evaluating the regional hydrologic impacts of global climatic changes. *Journal of Hydrology*, *88*(1–2), 97–116. https://doi.org/10.1016/0022-1694(86)90199-X

Hay, L. E., Wilby, R. L., & Leavesley, G. H. (2000). A COMPARISON OF DELTA CHANGE AND DOWNSCALED GCM SCENARIOS FOR THREE MOUNTAINOUS BASINS IN THE UNITED STATES 1. *JAWRA Journal of the American Water Resources Association*, *36*(2), 387–397. https://doi.org/10.1111/j.1752-1688.2000.tb04276.x

Hempel, S., K. Frieler, L. Warszawski, J. Schewe, and F. Piontek, 2013: A trend-preserving bias correction: The ISI-MIP approach. Earth Syst. Dyn., 4, 219–236, https://doi.org/10.5194/esd-4-219-2013.

Lange, S. (2019). Trend-preserving bias adjustment and statistical downscaling with ISIMIP3BASD (v1.0). Geoscientific Model Development, 12(7), 3055–3070. https://doi.org/10.5194/gmd-12-3055-2019

Lange, S. 2021: ISIMIP3BASD v2.5.0, https://doi.org/10.5281/zenodo.4686991

Maraun, D. (2016). Bias Correcting Climate Change Simulations - a Critical Review. *Current Climate Change Reports*, *2*(4), 211–220. https://doi.org/10.1007/s40641-016-0050-x

Mehrotra, R., & Sharma, A. (2012). An improved standardization procedure to remove systematic low frequency variability biases in GCM simulations. *Water Resources Research*, *48*(12), 1–8. https://doi.org/10.1029/2012WR012446

Mehrotra, R., & Sharma, A. (2016). A Multivariate Quantile-Matching Bias Correction Approach with Auto- and Cross-Dependence across Multiple Time Scales: Implications for Downscaling. *Journal of Climate*, *29*(10), 3519–3539. https://doi.org/10.1175/JCLI-D-15-0356.1

Muhamad Ali, M. M. A., & Othman, F. (2017). Selection of variogram model for spatial rainfall mapping using Analytical Hierarchy Procedure (AHP). Scientia Iranica, 24(1), 28-39. https://doi.org/10.24200/sci.2017.2374.

Benjamin Murphy, Roman Yurchak, & Sebastian Müller. (2022). GeoStat-Framework/PyKrige: v1.7.0 (v1.7.0). Zenodo. https://doi.org/10.5281/zenodo.7008206

Peter, J., Vogel, E., Sharples, W., Bende-Michl, U., Wilson, L., Hope, P., Dowdy, A., Kociuba, G., Srikanthan, S., Duong, V. C., Roussis, J., Matic, V., Khan, Z., Oke, A., Turner, M., Baron-Hay, S., Johnson, F., Mehrotra, R., Sharma, A., Thatcher, M., Azarvinand, A., Thomas, S., Boschat, G., Donnelly, C., and Argent, R. 2023: Continental-scale bias-corrected climate and hydrological projections for Australia, Geosci. Model Dev. Discuss. [preprint], https://doi.org/10.5194/gmd-2023-7.

Pierce, D. W., Cayan, D. R., Maurer, E. P., Abatzoglou, J. T., & Hegewisch, K. C. (2015). Improved Bias Correction Techniques for Hydrological Simulations of Climate Change. *Journal of Hydrometeorology*, *16*(6), 2421–2442. https://doi.org/10.1175/JHM-D-14-0236.1

Switanek, M.B., Troch, P.A., Castro, C.L., Leuprecht, A., Chang, H.- I., Mukherjee, R. and Demaria, E.M.C. (2017) Scaled distribution mapping: a bias correction method that preserves raw climate model projected changes. Hydrology and Earth System Sciences, 21, 2649–2666. https://doi.org/10.5194/hess-21-2649-2017.